

DAS and DTS Monitoring at MiDAS Taiwan 井下光纖於米崙斷層的觀測研究及未來應用

馬國鳳(Kuo-Fong Ma^{1, 2}), and MiDAS team

¹Institute of Earth Science, Academia Sinica ²E-DREaM Center, National Central University, TAIWAN







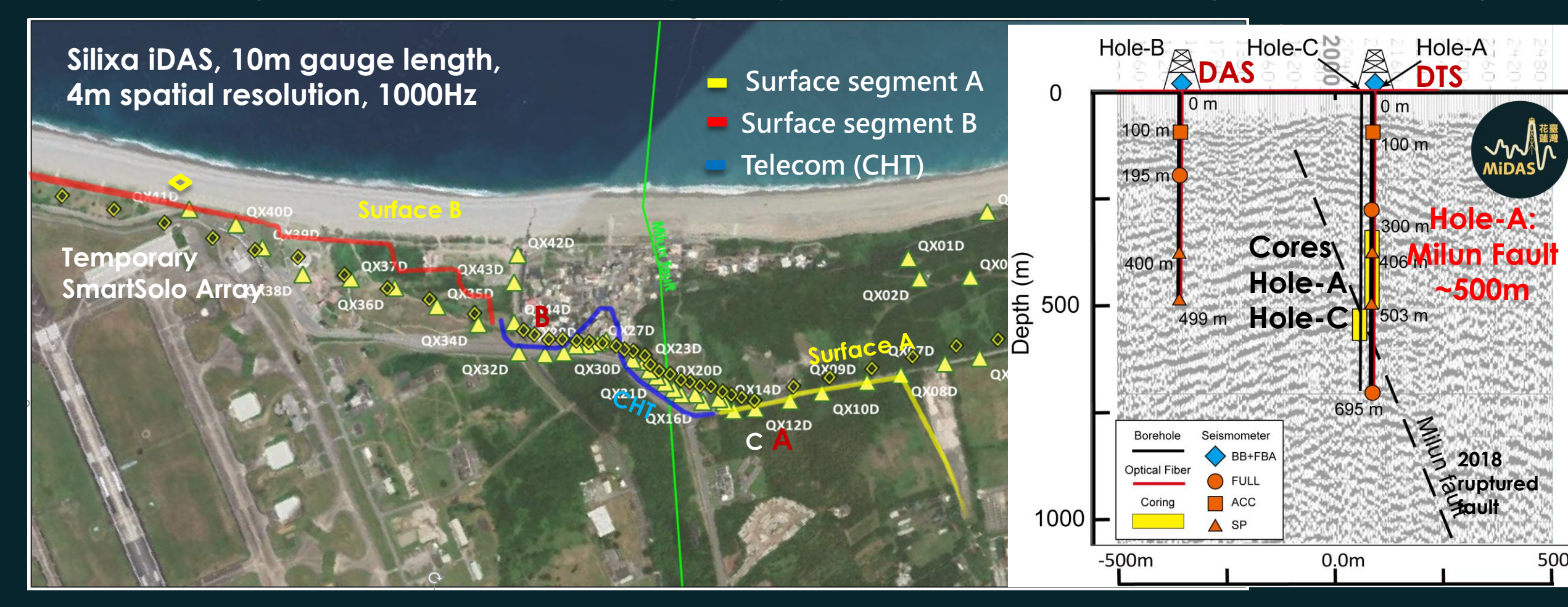


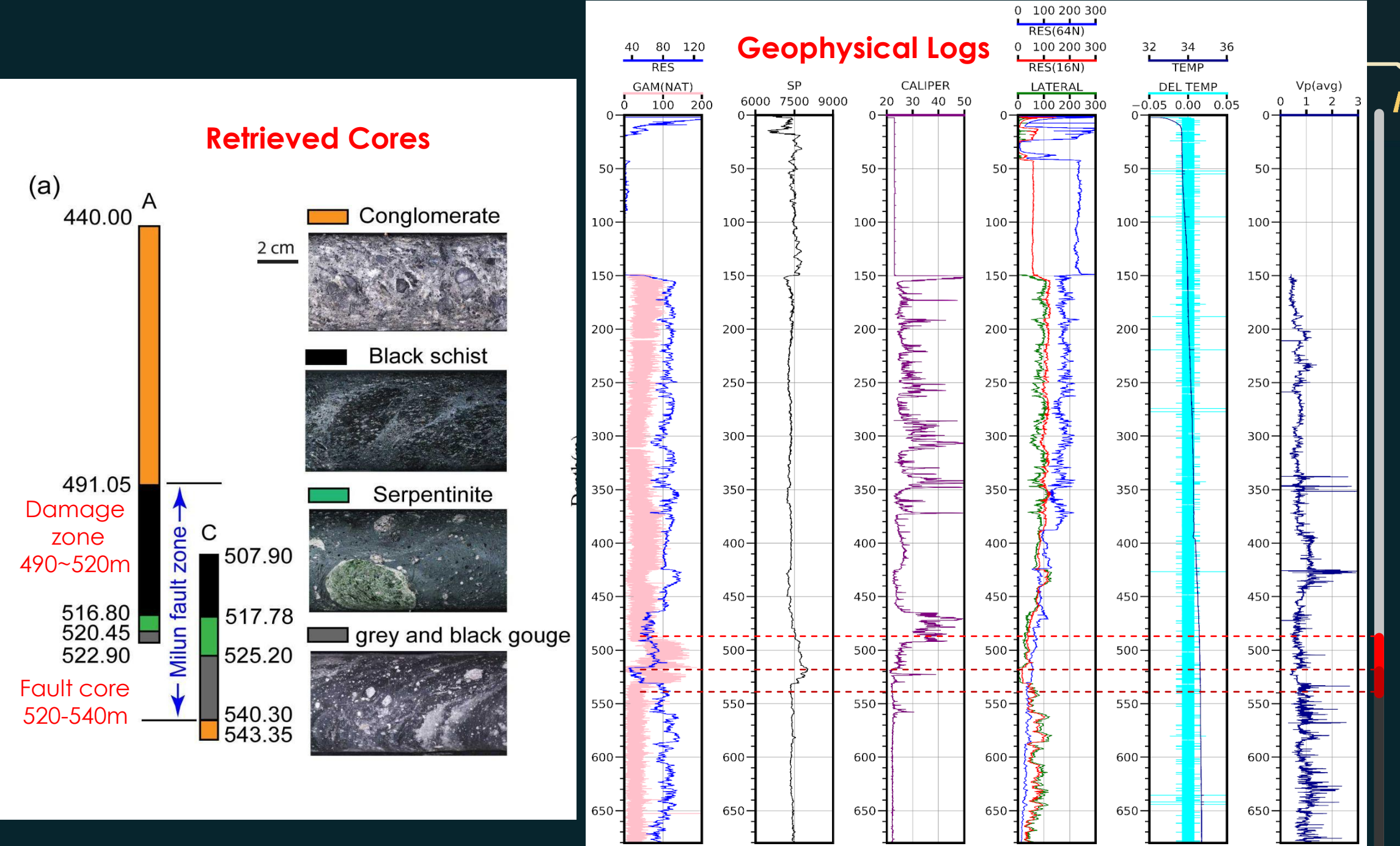
Milun fault Drilling and All-inclusive Sensing (MiDAS) crossing fault holes: 700m Hole-A, footwall 500m Hole-B



Hole-C: Fluid and gas monitoring

Crossing fault three-dimensional optical fiber configuration (HoleA, 0-700m-0, Surface A (forth-345m-back), Commercial Telecom, CHT (1052m), HoleB, 0-500m-0, Surface B (forth-1128m-back)







conglomerate

Damage zone fault core

solidated conglomerate

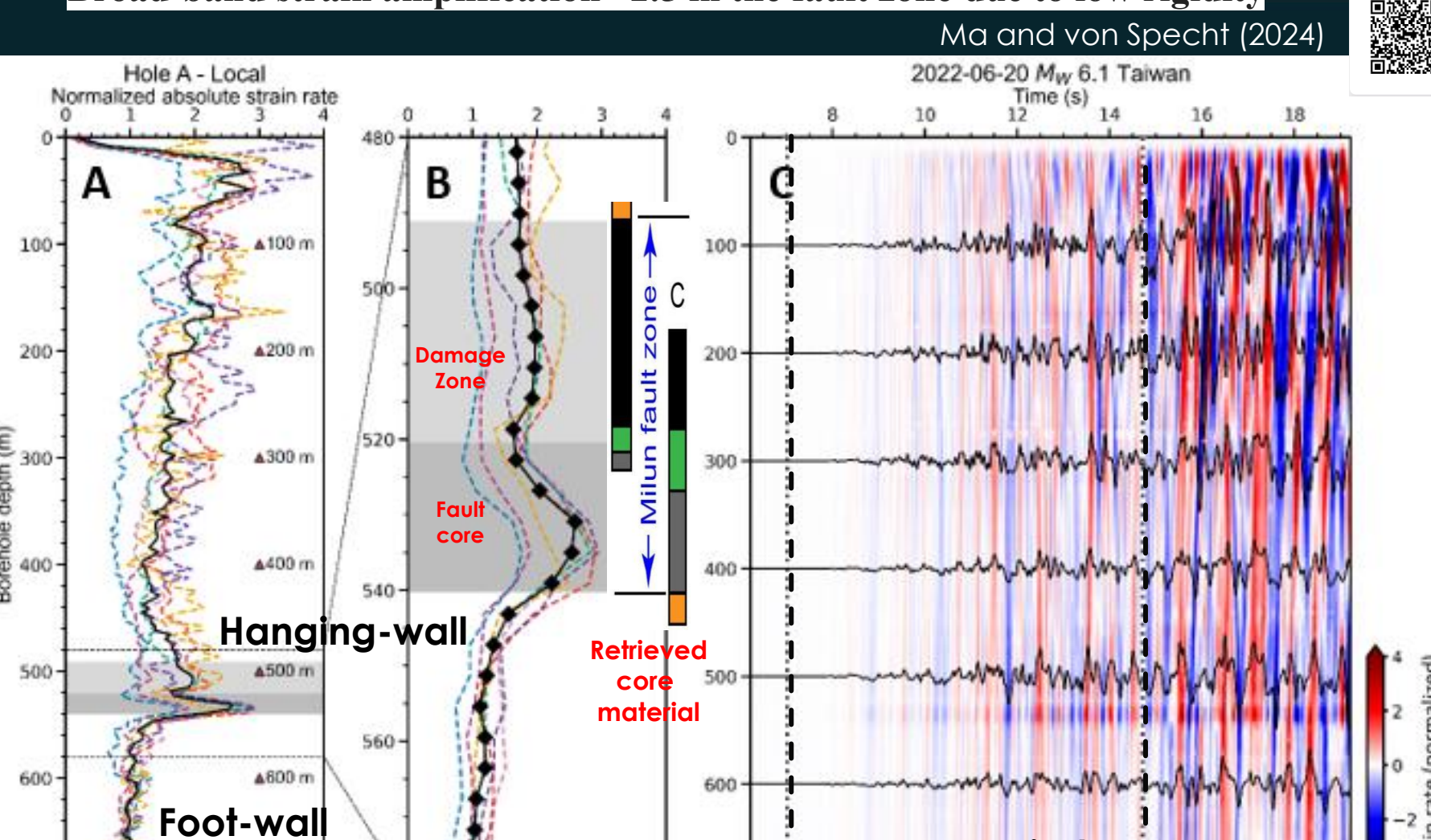
119°E 120°E 121°E Taiwan Strait 6.0 6.5 7.0 7.5 8.0 M_w 23°N Philippine

DAS (Distributed Acoustic Sensing) strain observations are highly sensitive to changes in rigidity, which are influenced by fluid dynamics and temperature variations.

These parameters are critical for effective CCS (Carbon Capture and Storage) monitoring.

Downhole Crossing fault Fiber Sensing at depth Observation from Local Earthquakes

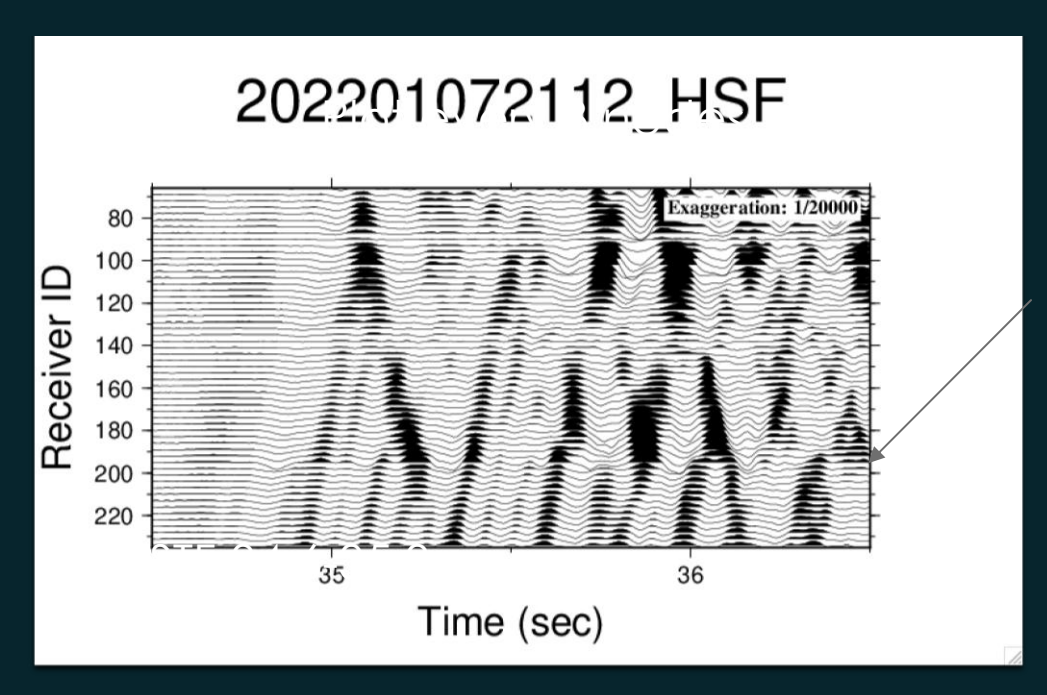
Broad-band strain amplification ~2.5 in the fault zone due to low rigidity



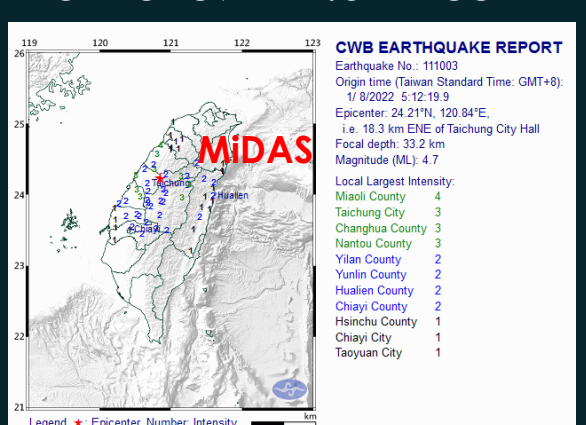
P-wave window!

How does strain (rate) vary across different lithological layers? (Identifying the lithological layers, for CCS monitoring, using event based and ambient noise)





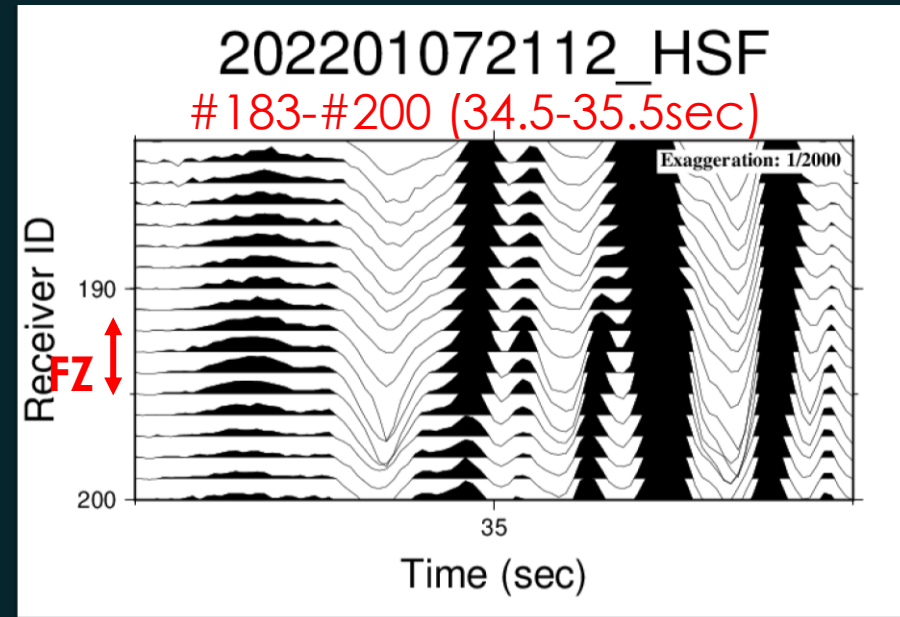
Direct Observation by DAS at Hole-A 20220107 M4.6 D~33km



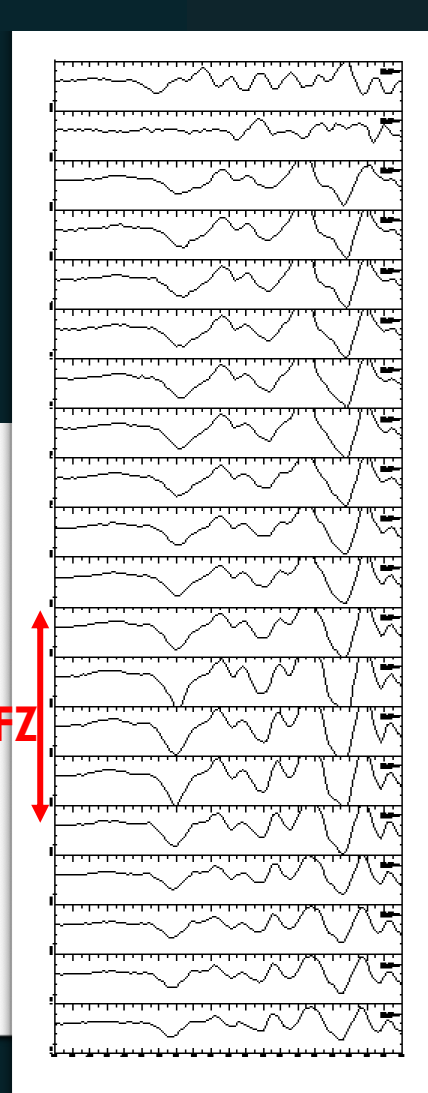
Sediment thickness
Disturbance in waves (Fracture Zone?)

Major Fault Zone LVZ to amplify the phases

More consistent features in the footwall



FZ amplification, and change in period Fault Zone, 520-540m~ 20m

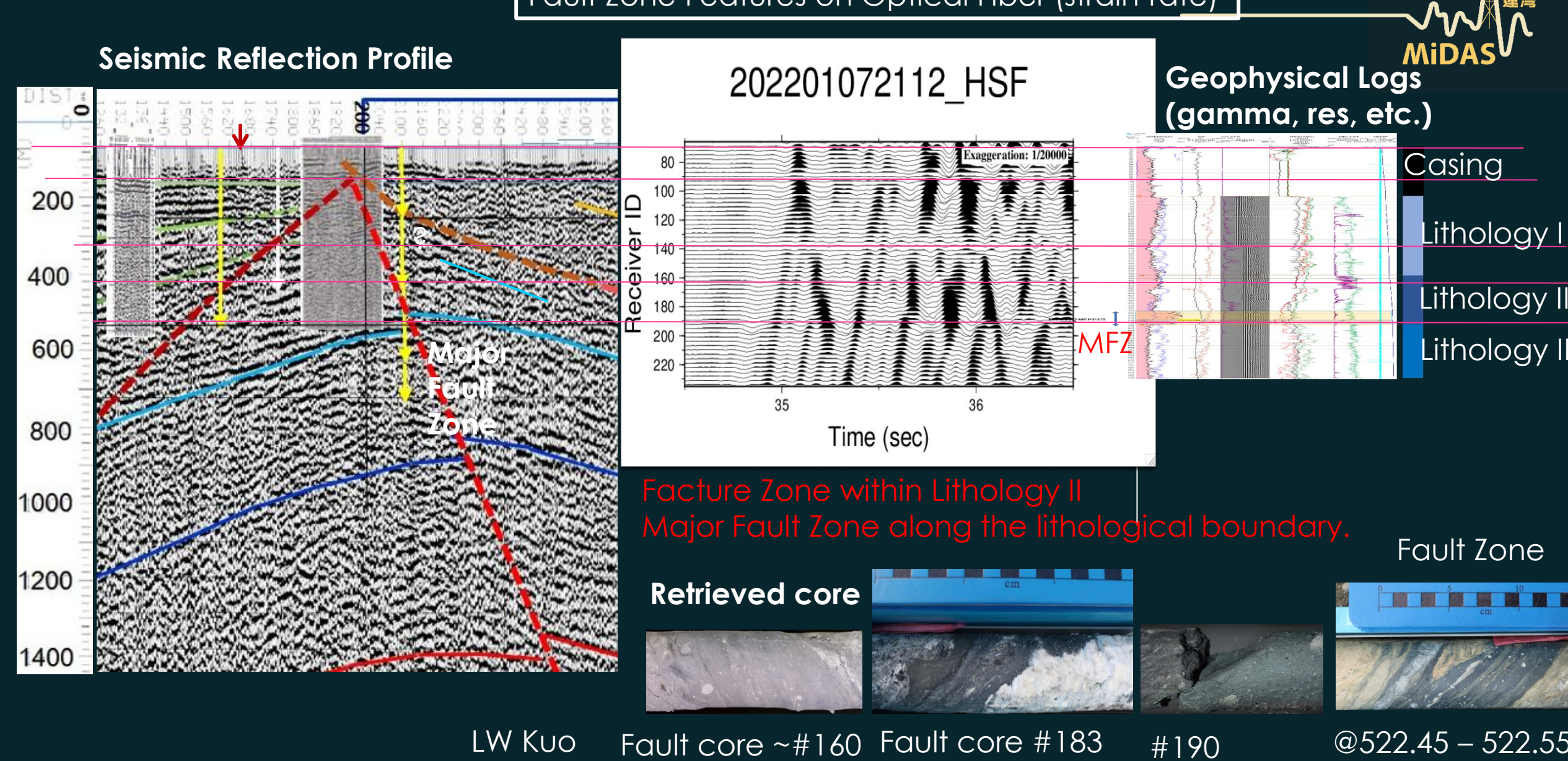


Fault Zone Features on Optical Fiber (strain-rate)

@491.05 - 491.15

~#192

@516.70-516.85

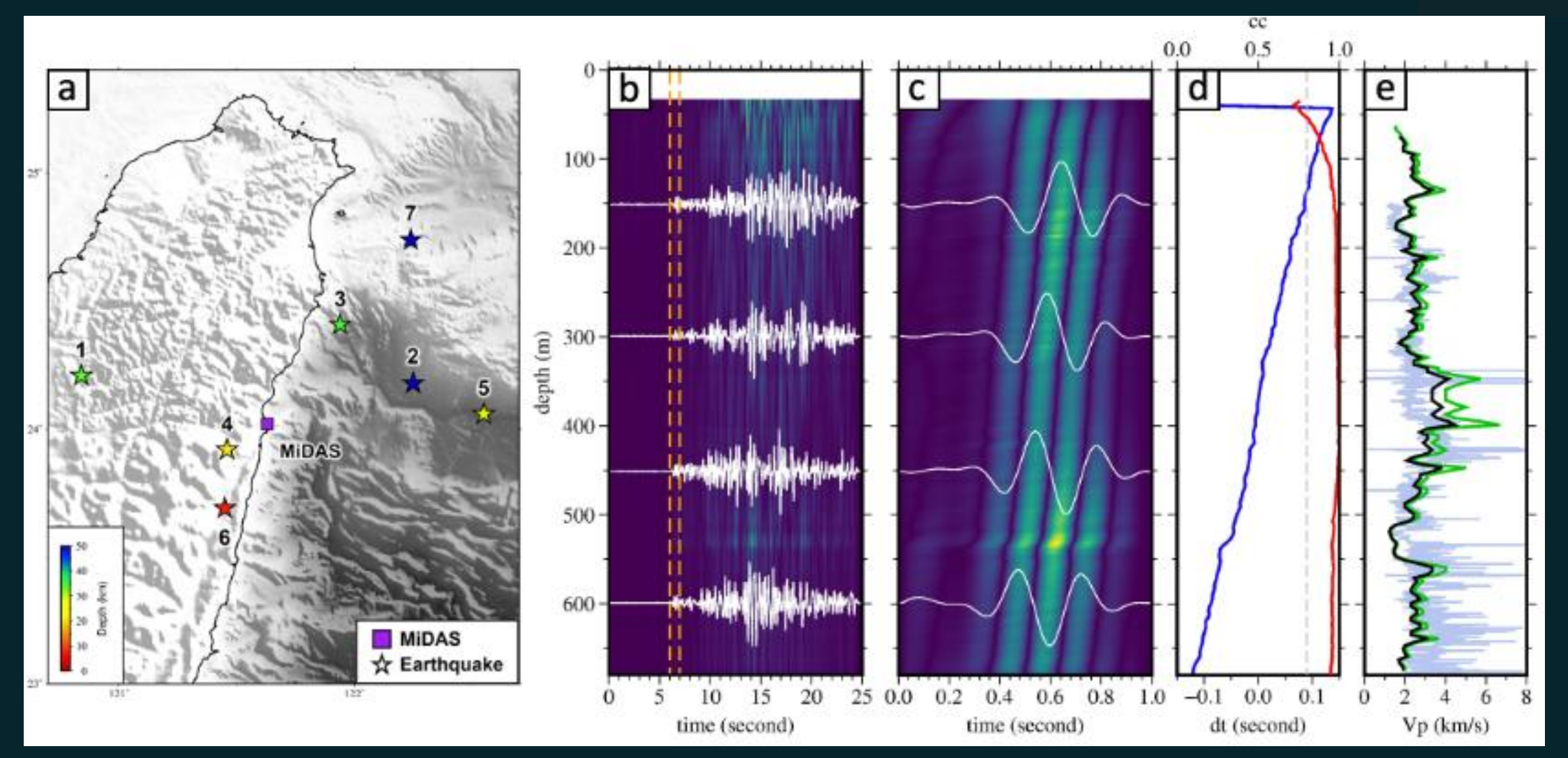


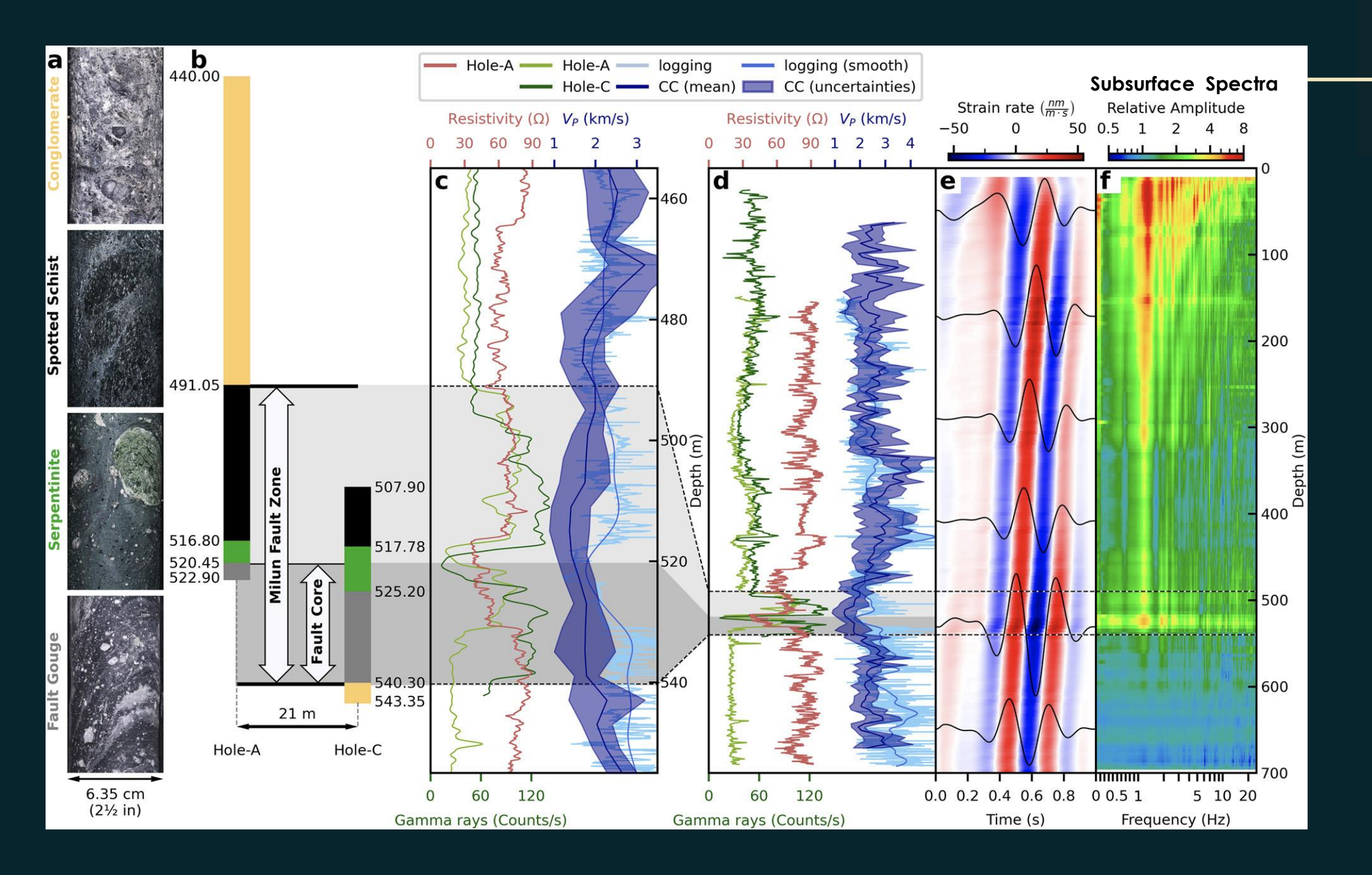
@426m

WJ Wu

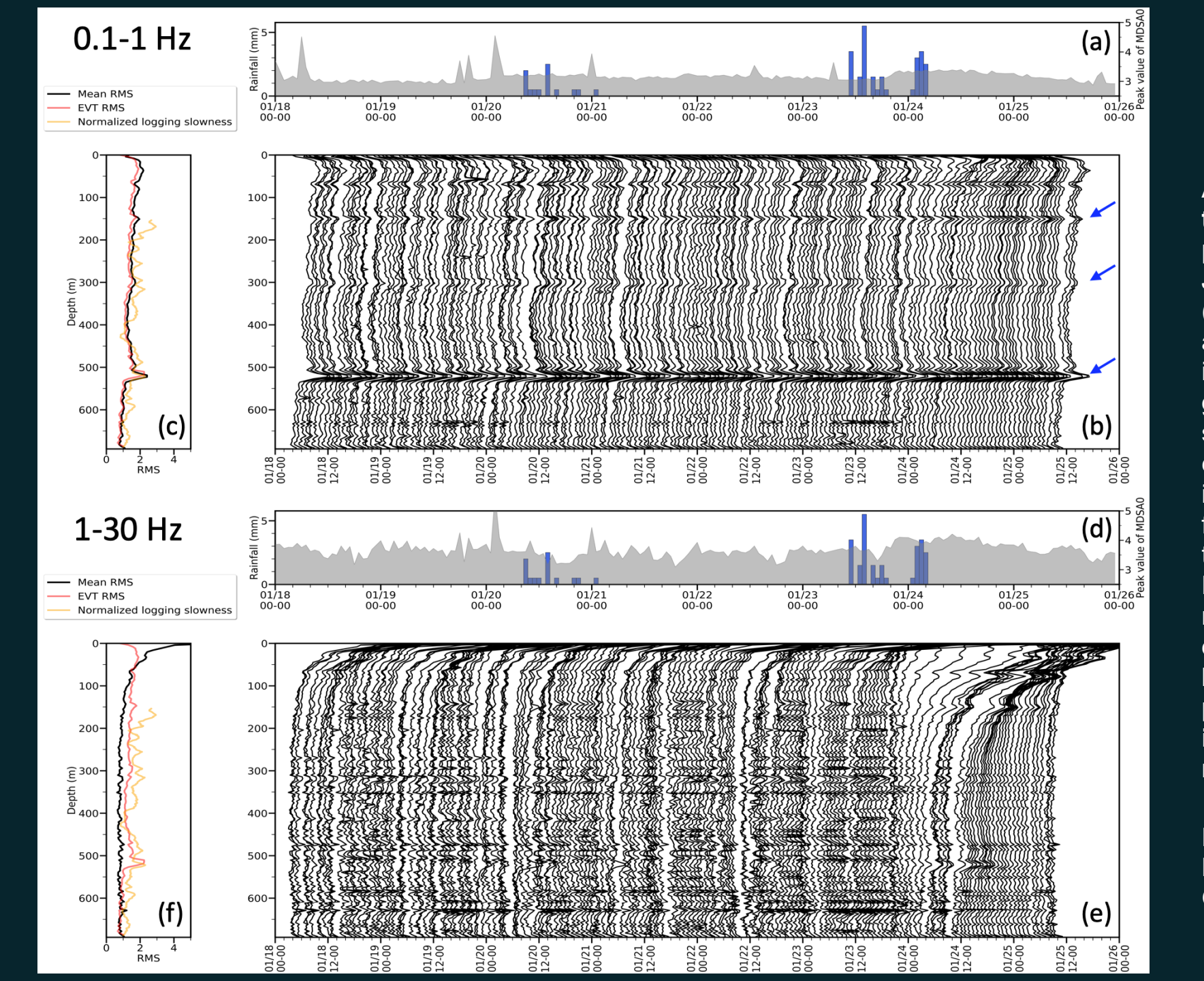
Sensing fault zone velocity structure using cross-correlation through downhole optical fiber













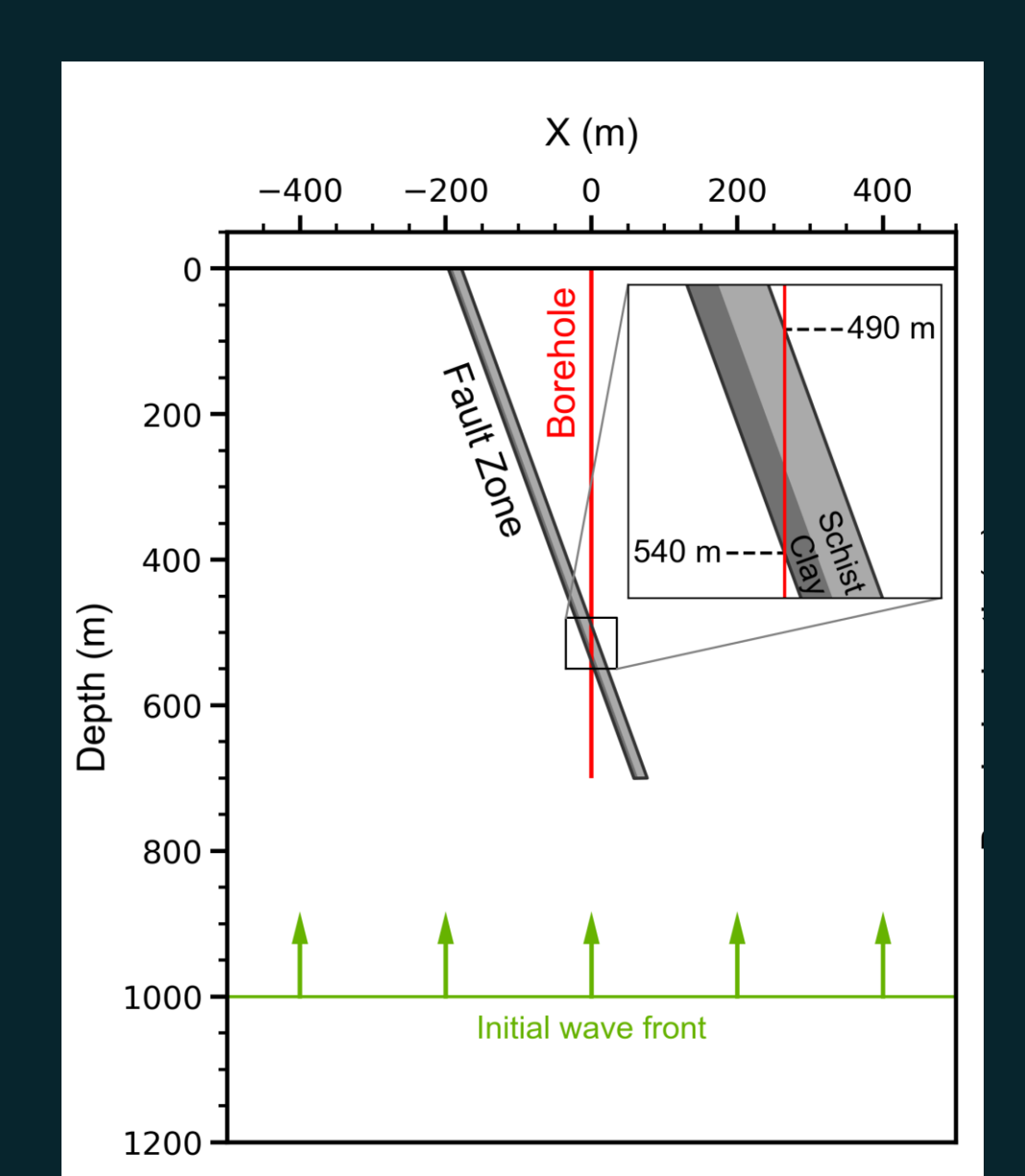
Ambient Noise Long-term temporal RMS amplitude ratio profiles at Hole A from 18-25 January 2023 in (a-c) 0.1-1 Hz and (d-f) 1-30 Hz frequency bands. (a) and (d) show the hourly precipitation in blue bars and the hourly peak ground motions in gray. (b) and (e) show the hourly moving-window calculation of RMS amplitude ratios in corresponding frequency bands. (c) and (f) show the comparison between the mean RMS amplitude ratio profile (black), mean RMS amplitude ratio profile derived from earthquakes, and logging P-wave slowness (1/velocity) profile (orange). Blue arrows indicate the low velocity zones or rigidity contrasts.

Huang, Ma et al. (AGU books, Distributed Acoustic Sensing in Borehole Geophysics, 2024)

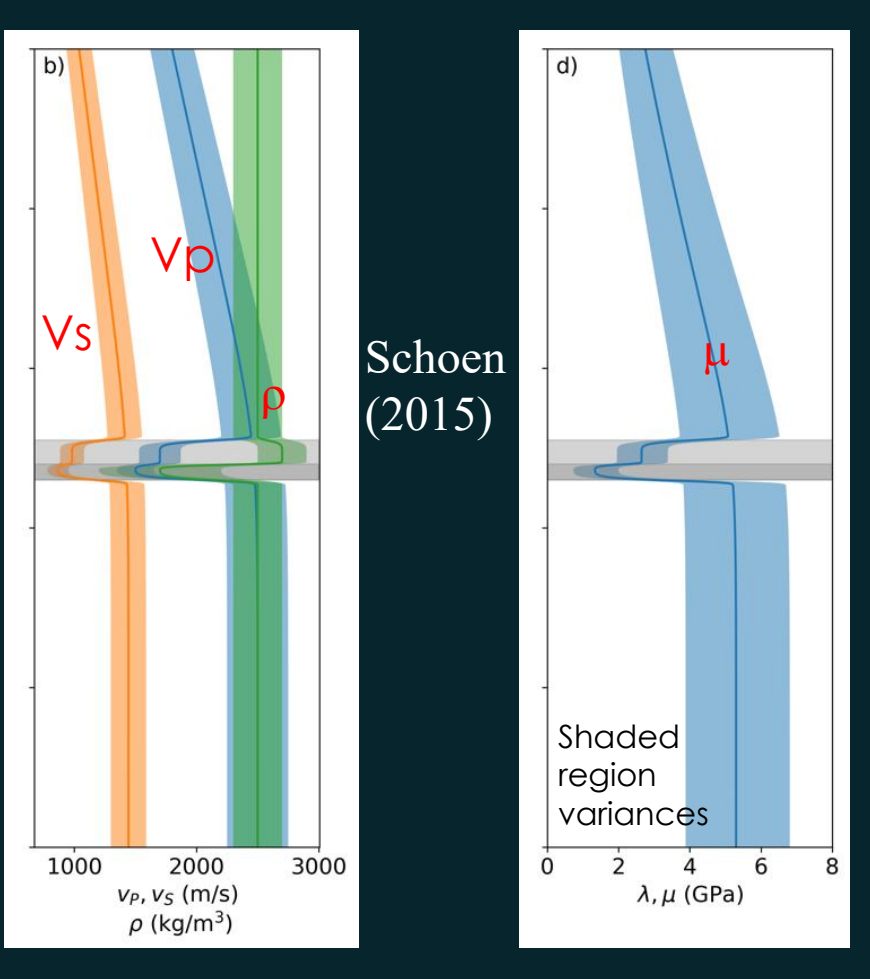
2D finite-difference simulation, heterogenous medium in elastic modulus,

dx=dy=2m; dt=0.00015 sec, Source Time Function, Gaussian derivative Velocity models with variances, Logging and OFS through CC





Velocity models, and elastic constant (rigidity) profile (Assuming Poisson material)



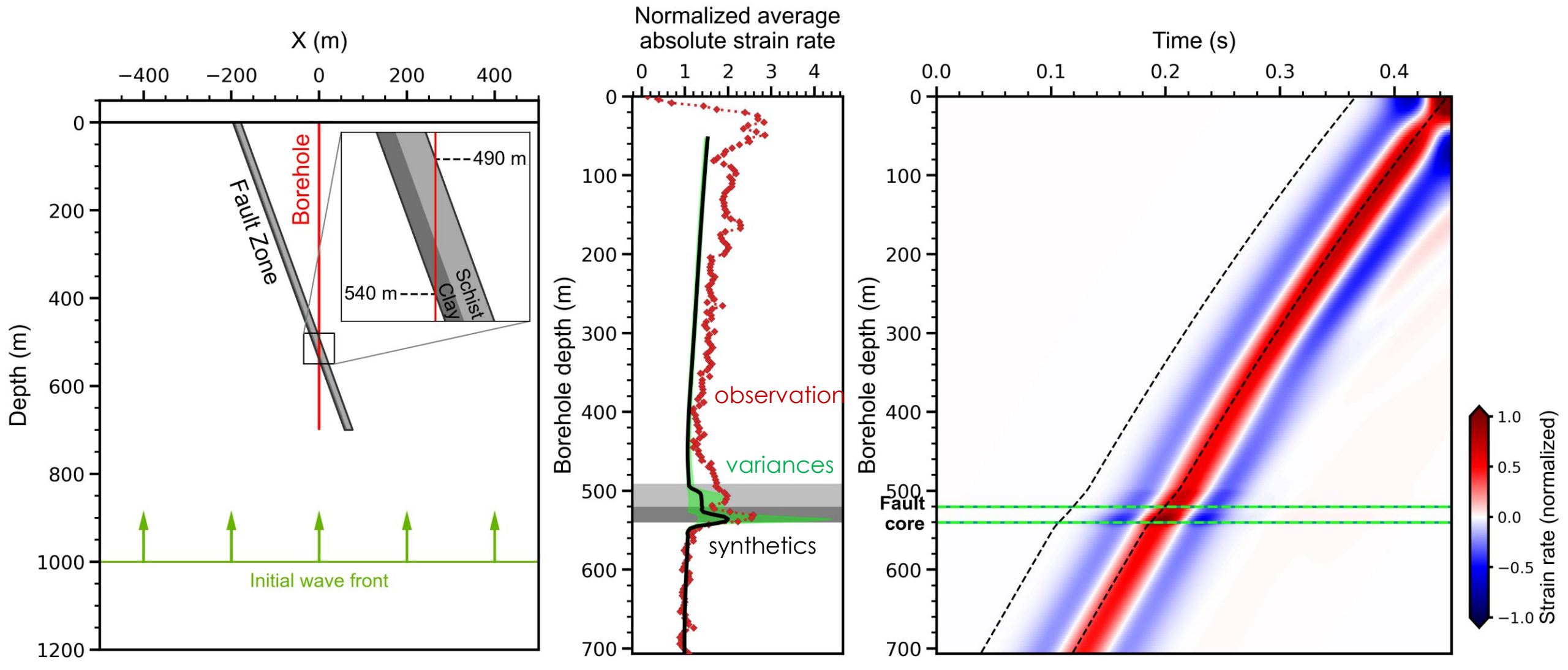
Reduction
within fault zone
Damage zone
Fault core

- Strain is sensitive to rigidity changes

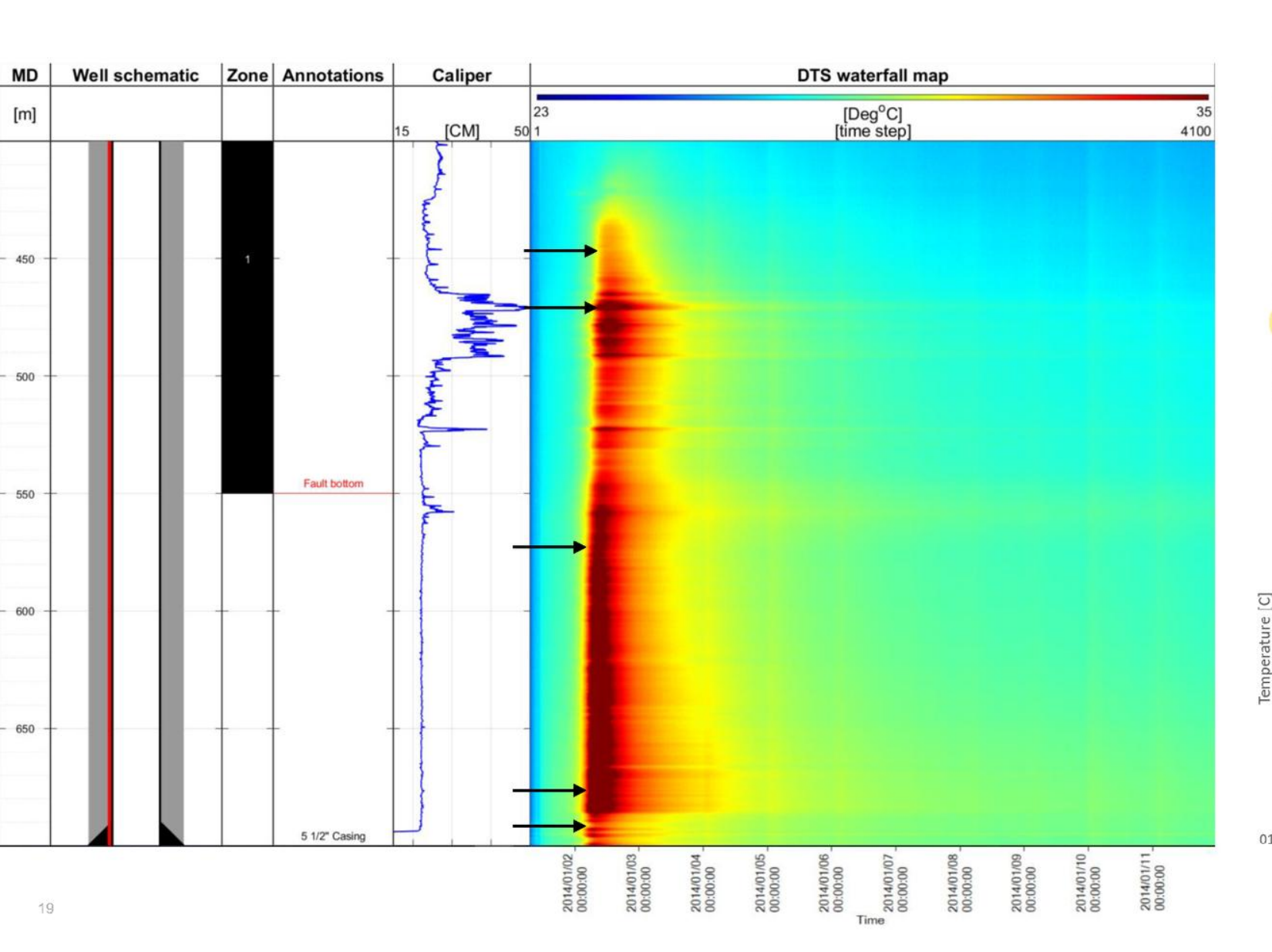
=> Optical fiber sesining for monitoring temporal rigidity changes (fluid, velocity changes, environment changes

Simulation results full displacement, taking temporal and spatial derivatives to strain-rate) MiD/





DTS combo plot caliper, DTS waterfall map and DTS traces - Zoom-in [400m to 700m]

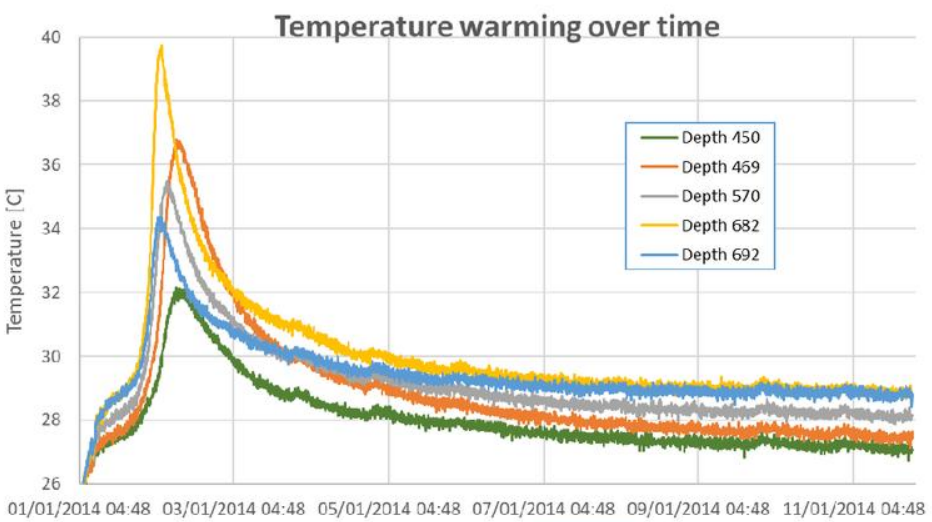


The following depths were selected to create a temperature warming over time comparison.

It can be noticed how after the cool-back [post cement curing warming] the temperatures go back to higher temperatures in the deepest points selected, which would agree with a vertical well temperature gradient.

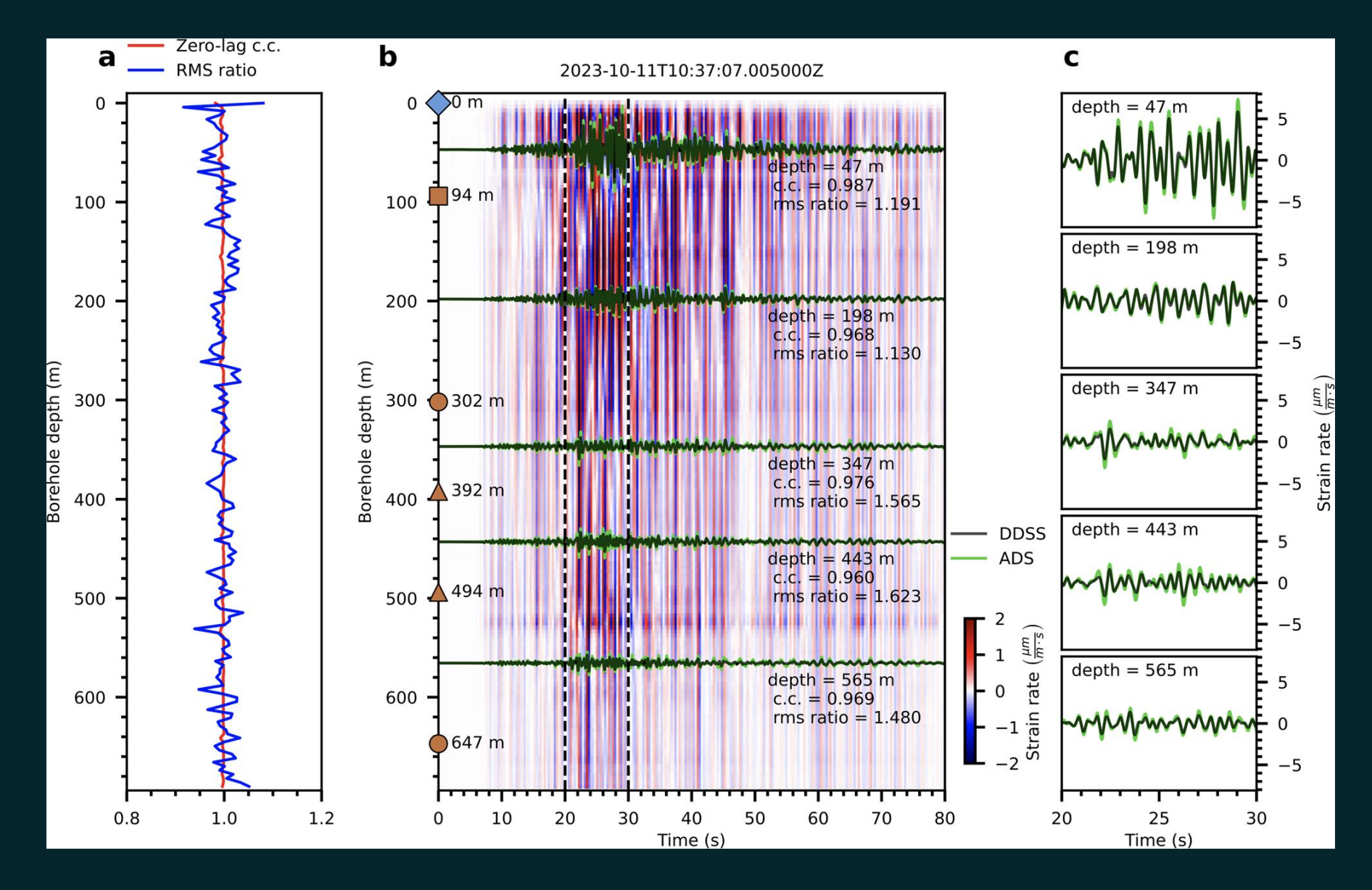
It can be appreciated that even though 469m is a shallower depth, this one reaches higher temperature warming during cement curing than 470m and 692m.

The depth that reaches the highest temperature can be seen at 682m.

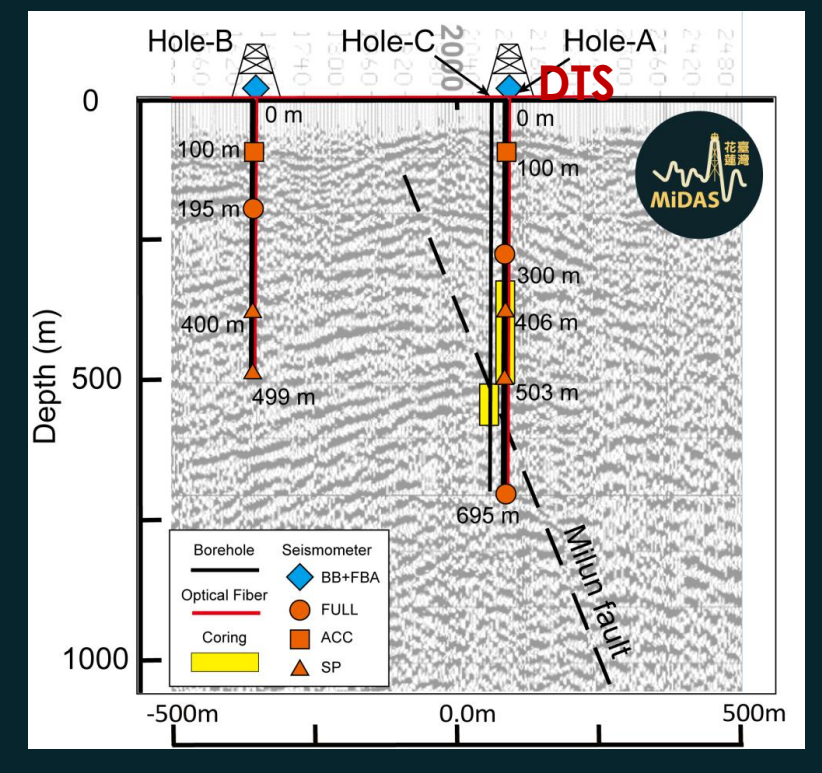


Reliability of the borehole optical fiber from DAS and seismic array derived strain: ensuring good quality of cementing and fading effects



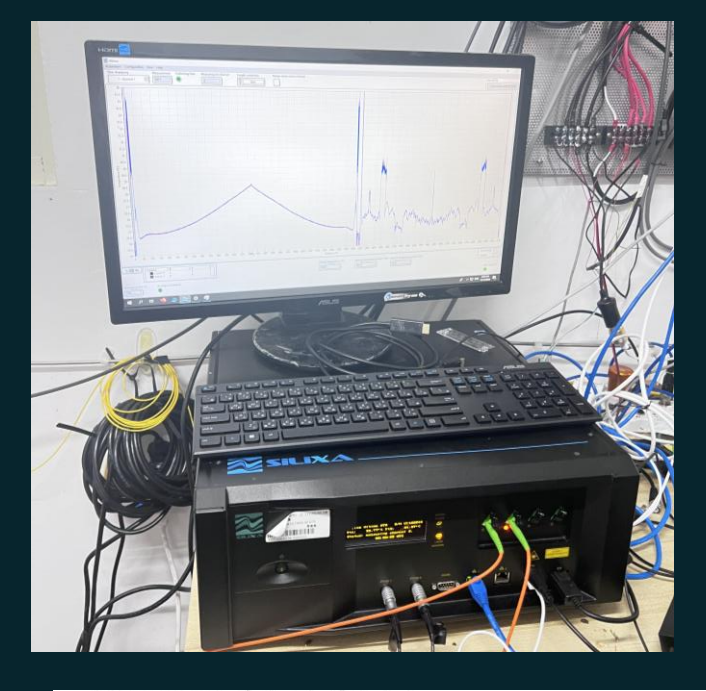


DAS/DTS observatory

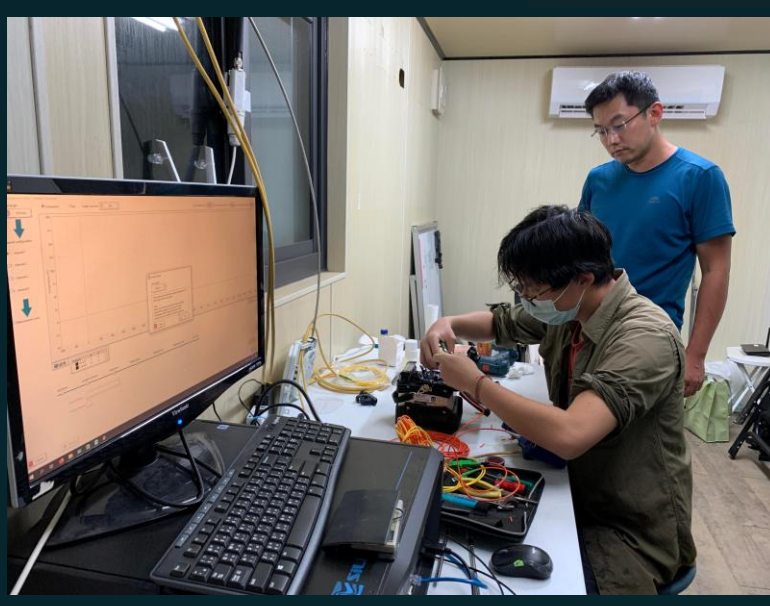




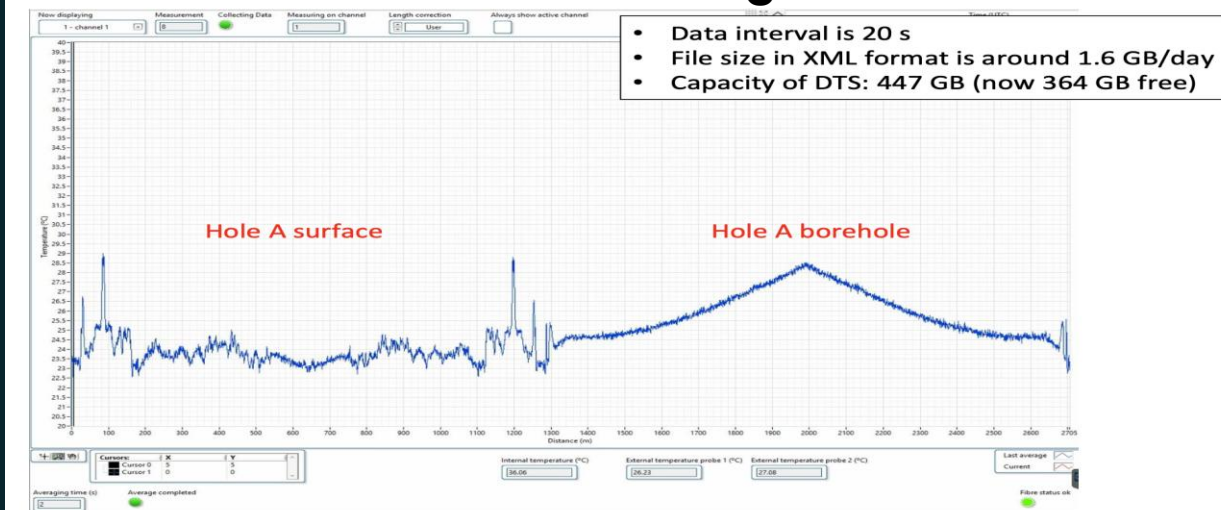
DTS @Hole-A (0.254 m SR, 20sec SR)



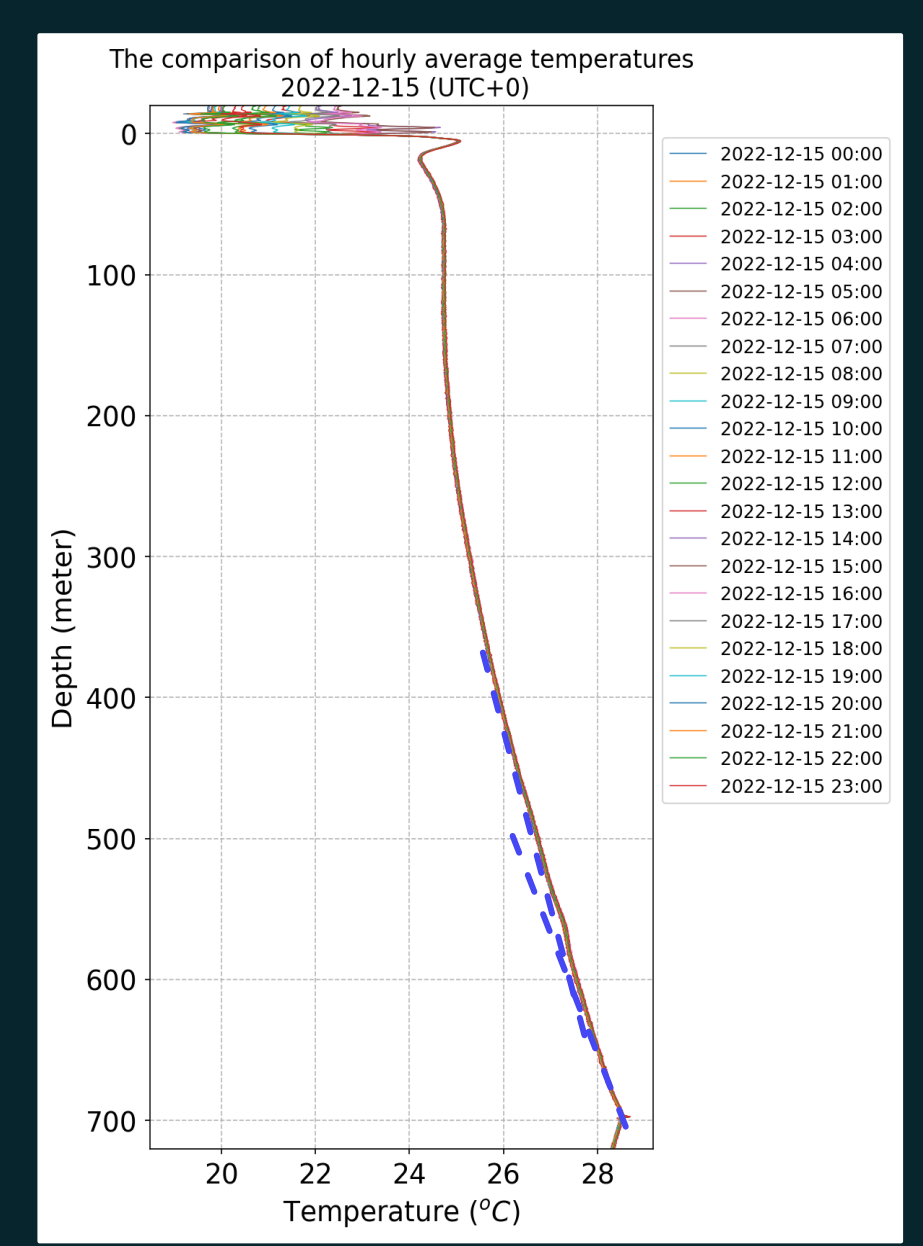
Final splicing for DAS loops

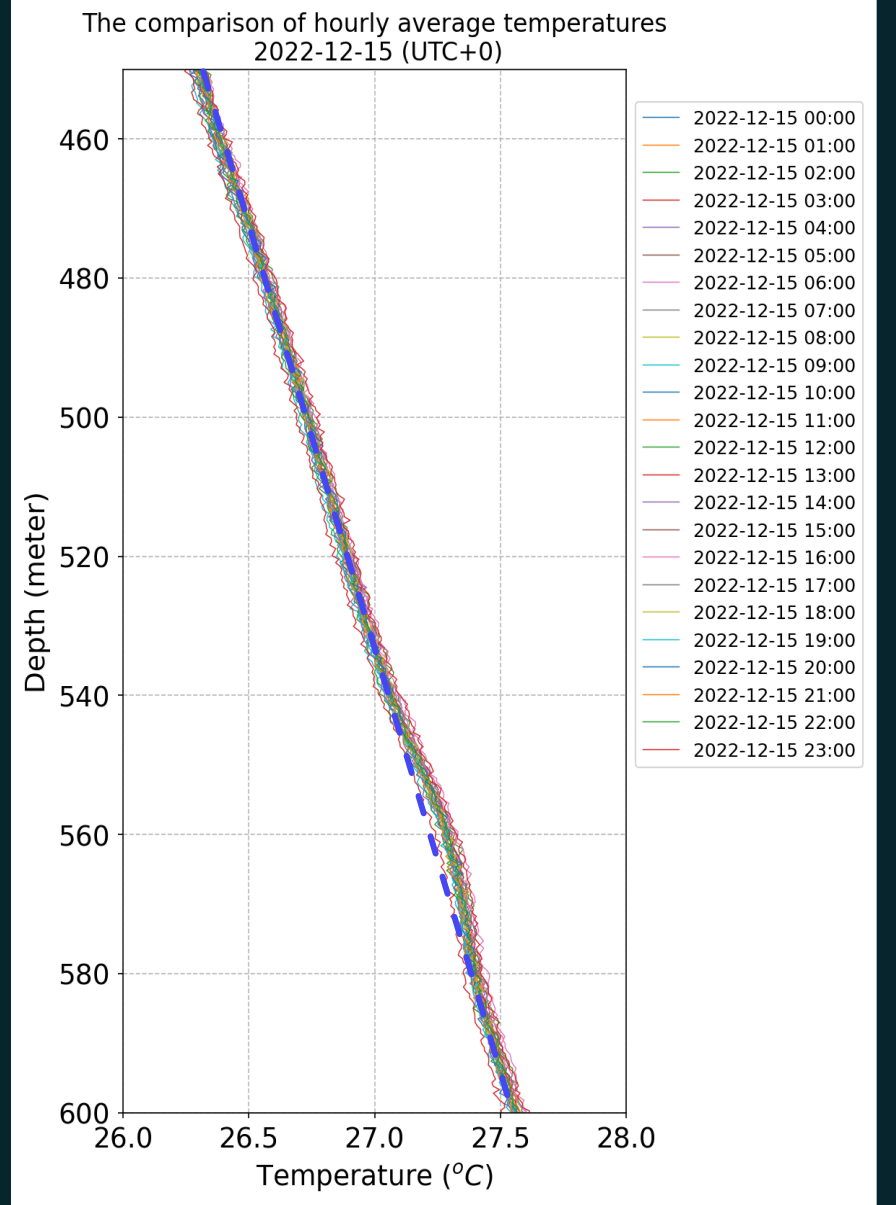


2022/11/15 DTS monitoring



DTS hourly average temperature profile

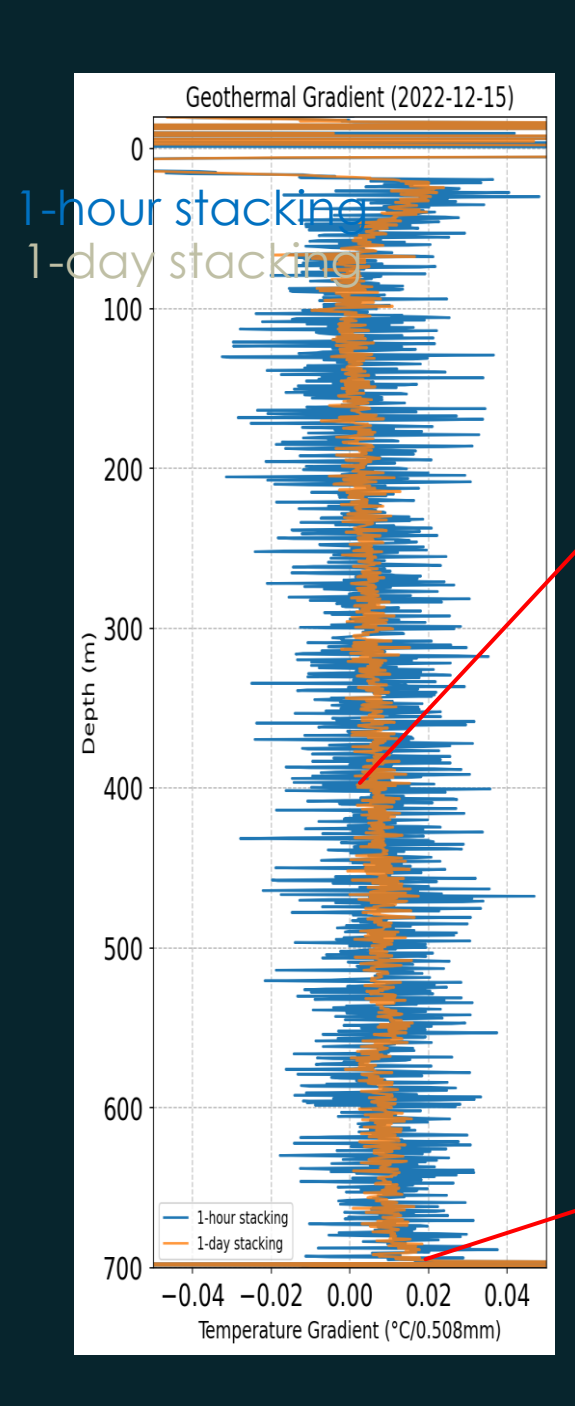




Background geothermal gradient

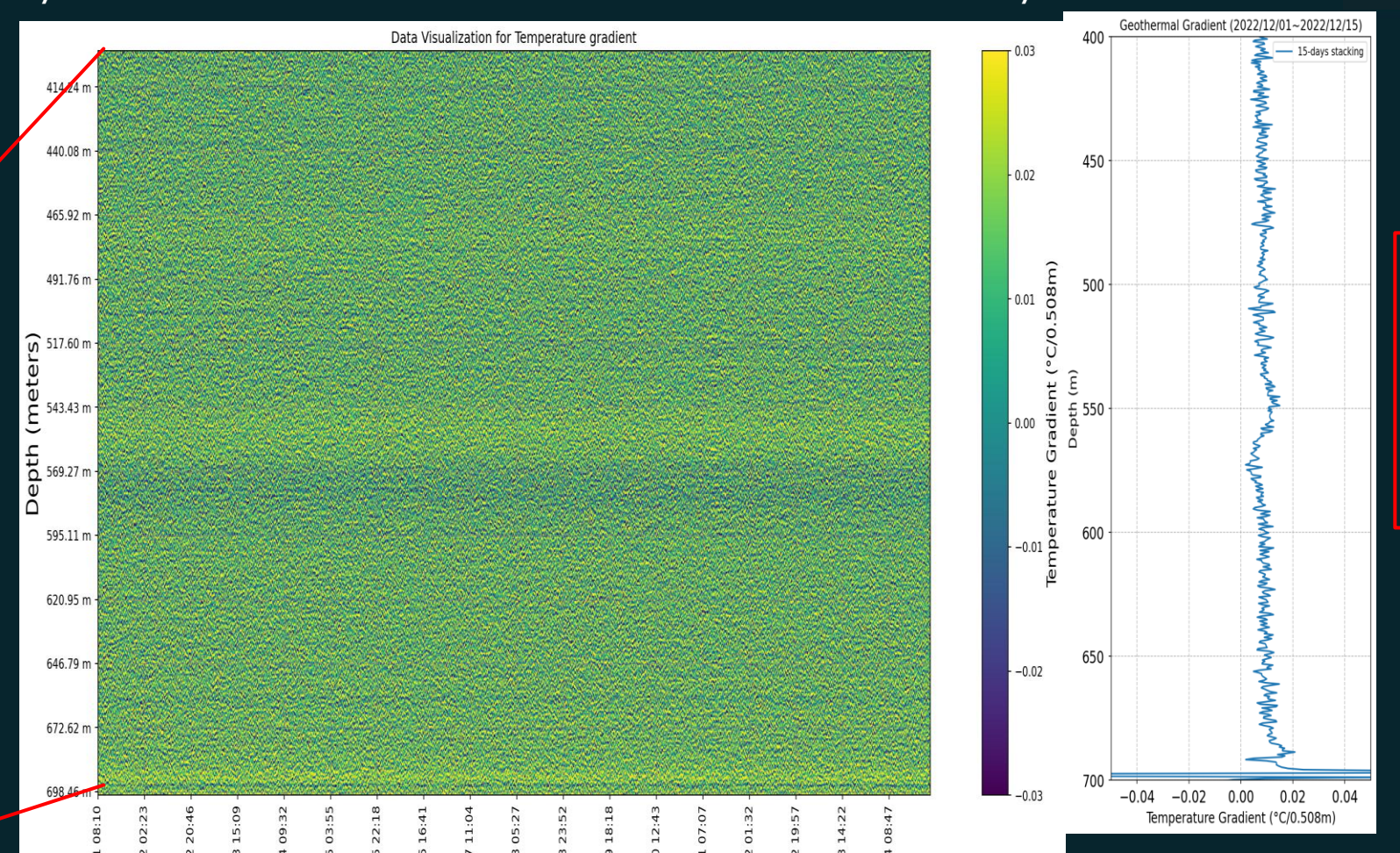
- Top 150m, environmental influence
- Disturbance deeper than 150m, might be crustal related features
- Nonlinear geothermal gradient
- The average temperature profile is rather stable regardless the variations with and without controlled head temperature
- Subtle temperature anomaly within the range of 550-580m
- Subtle geothermal gradient changes above and below the fault gouge zone

The changes in acothormal



Geothermal gradient map in the depth of 400-700 m (2022/12/01~12/14)





15-days sta

Geothermal Gradient changes below MFZ within the range of 540-580m

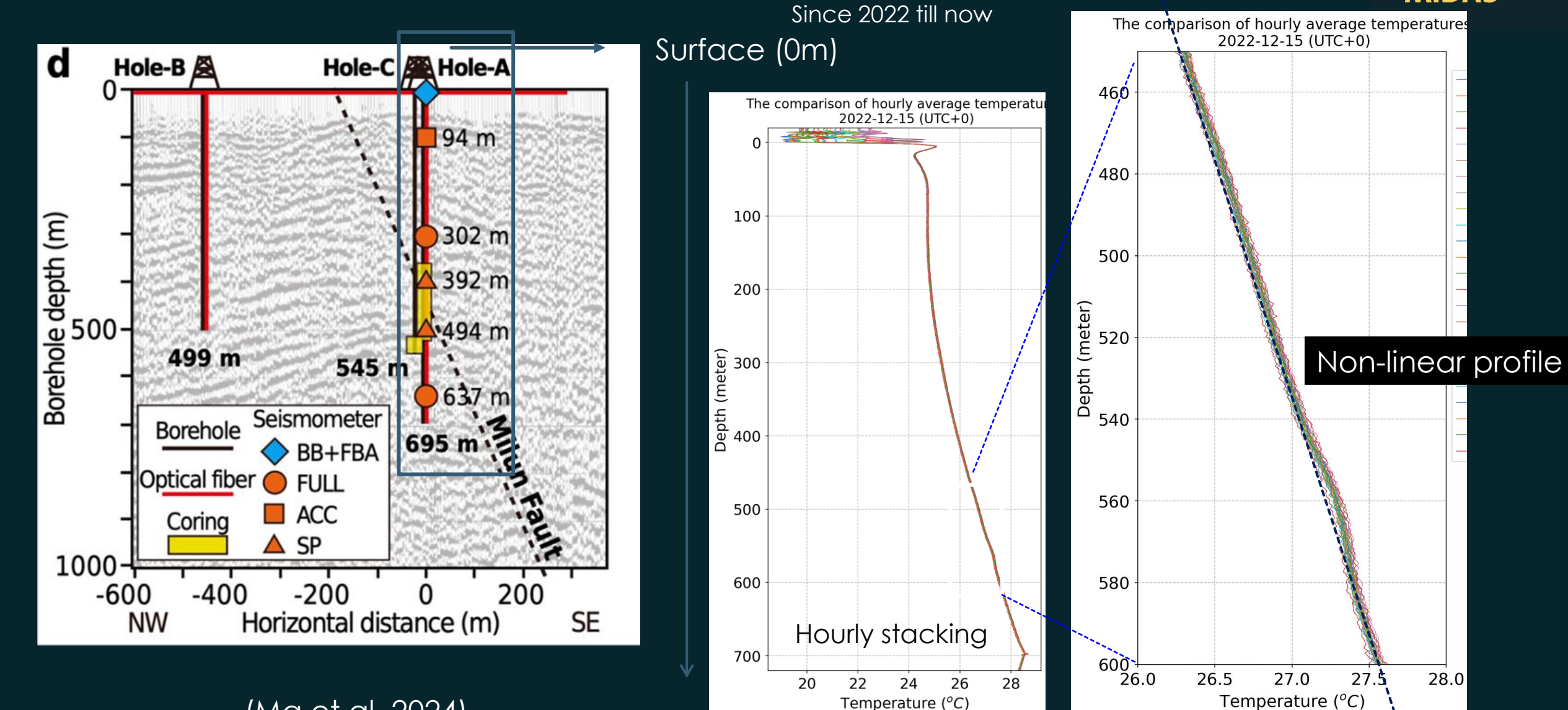
Borehole temperature profile in Hole-A • Depth resolution: 0.245 m Distributed Temperature Sensing (DTS)

(Ma et al, 2024)

Temp. resolution: 0.01 °C



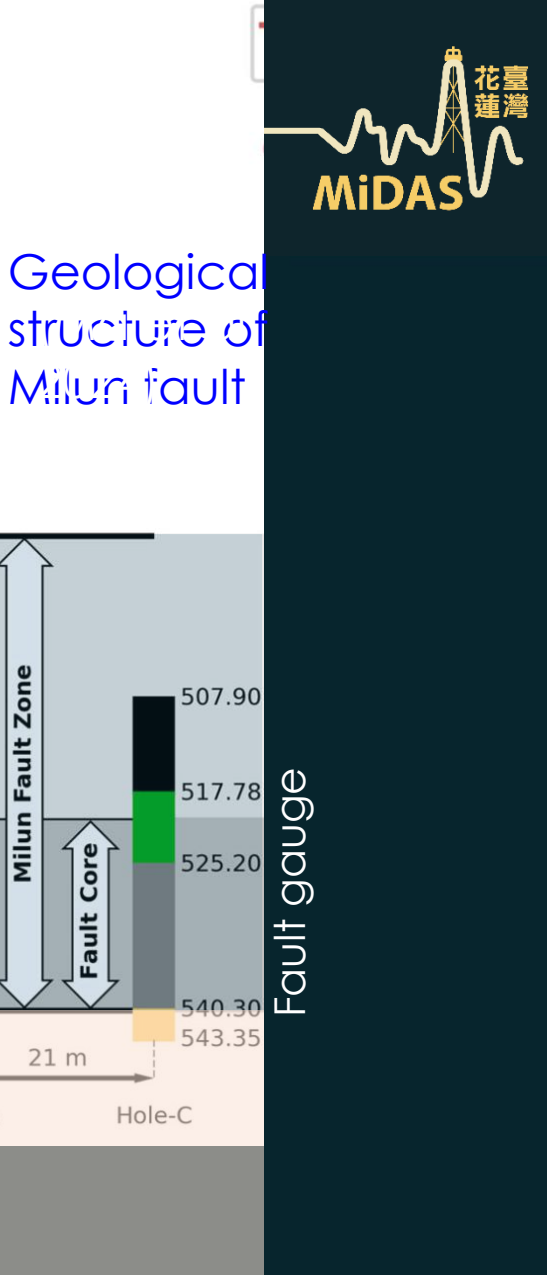
28.0



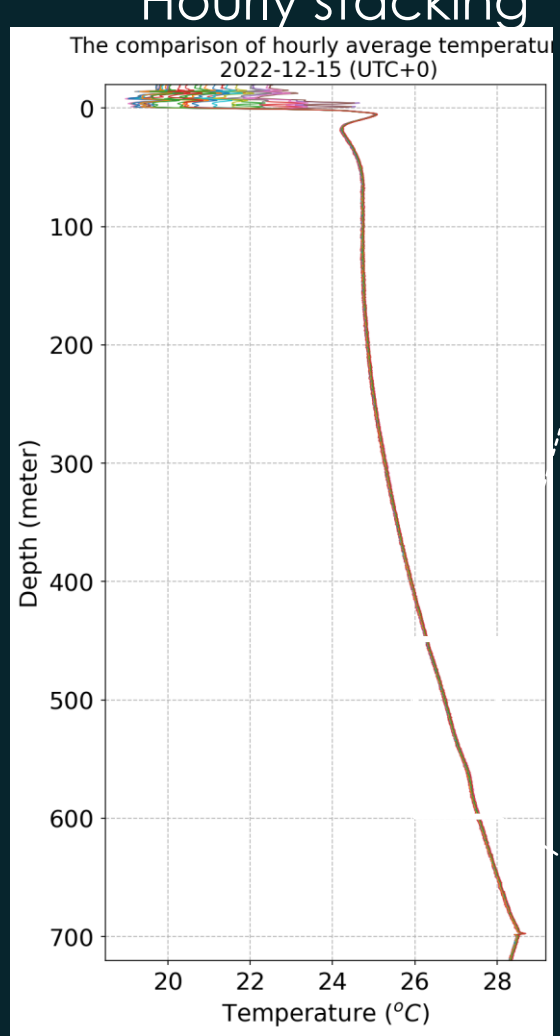
Bottom (675m)

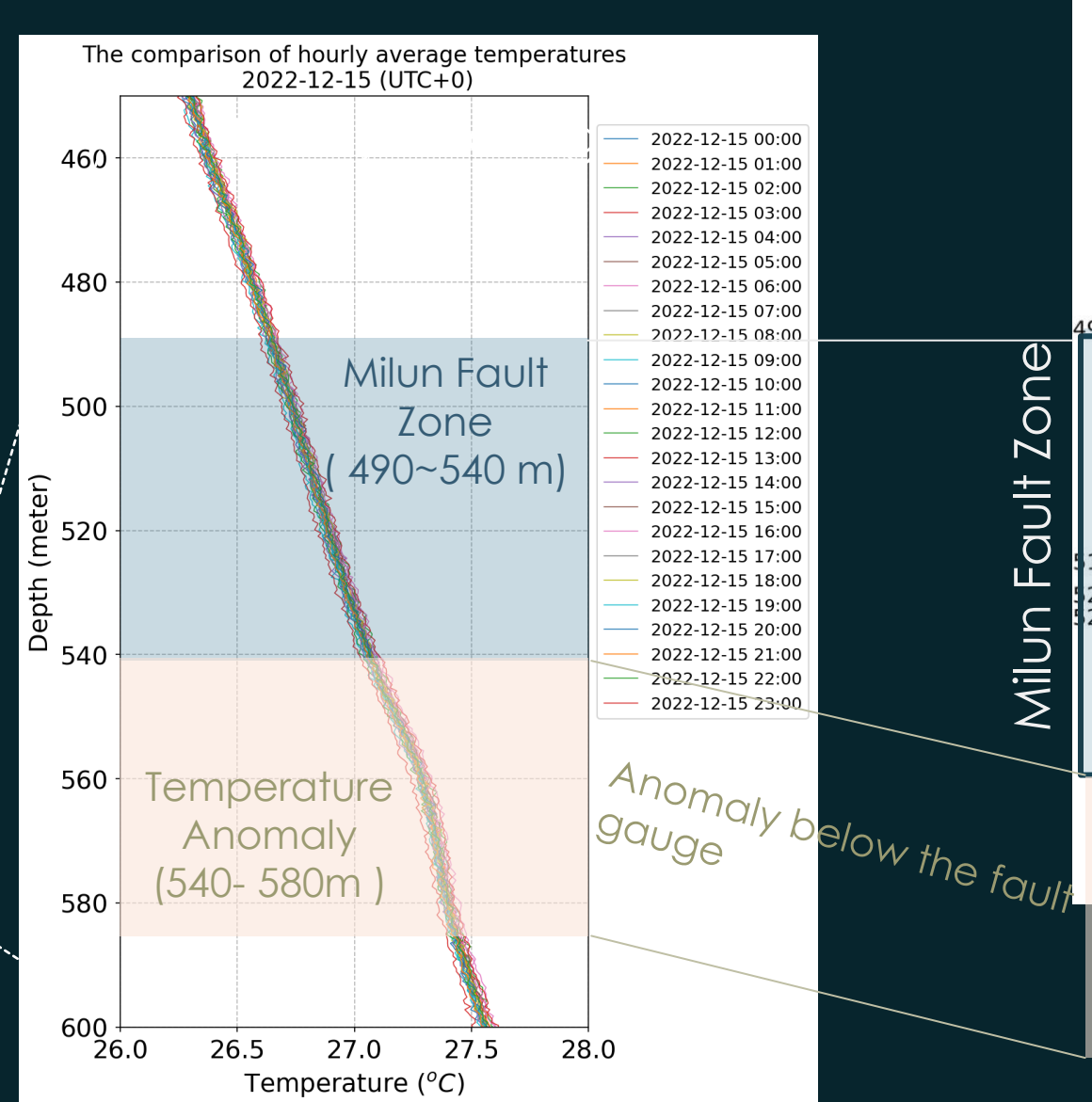
Hsian-Ting Lai TGA/ 2025.06.17

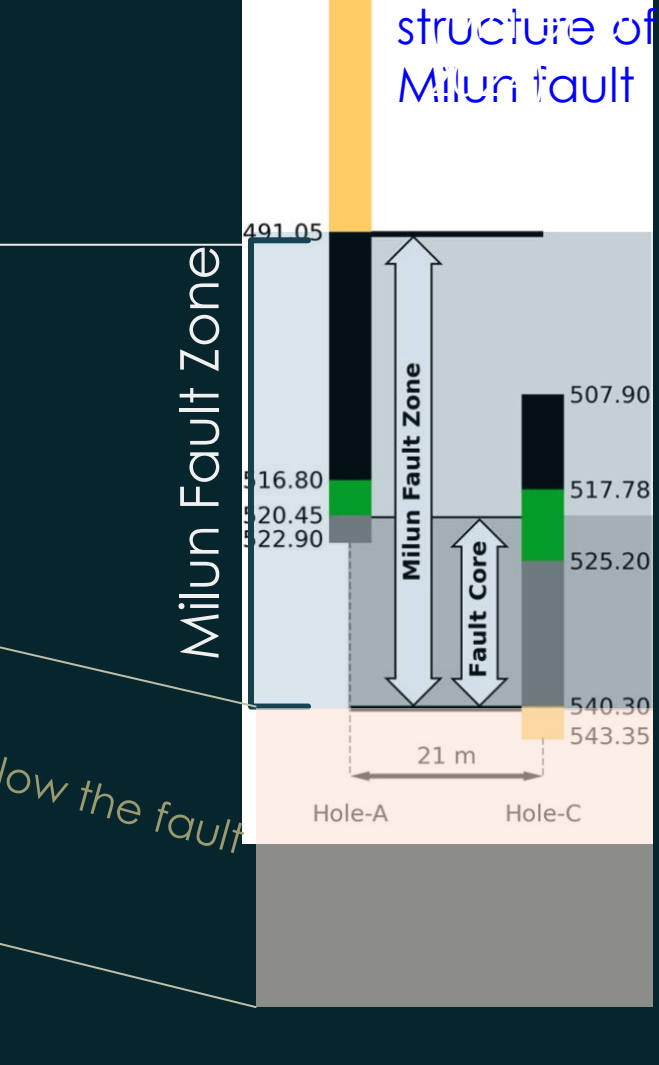
DTS hourly average temperature profile





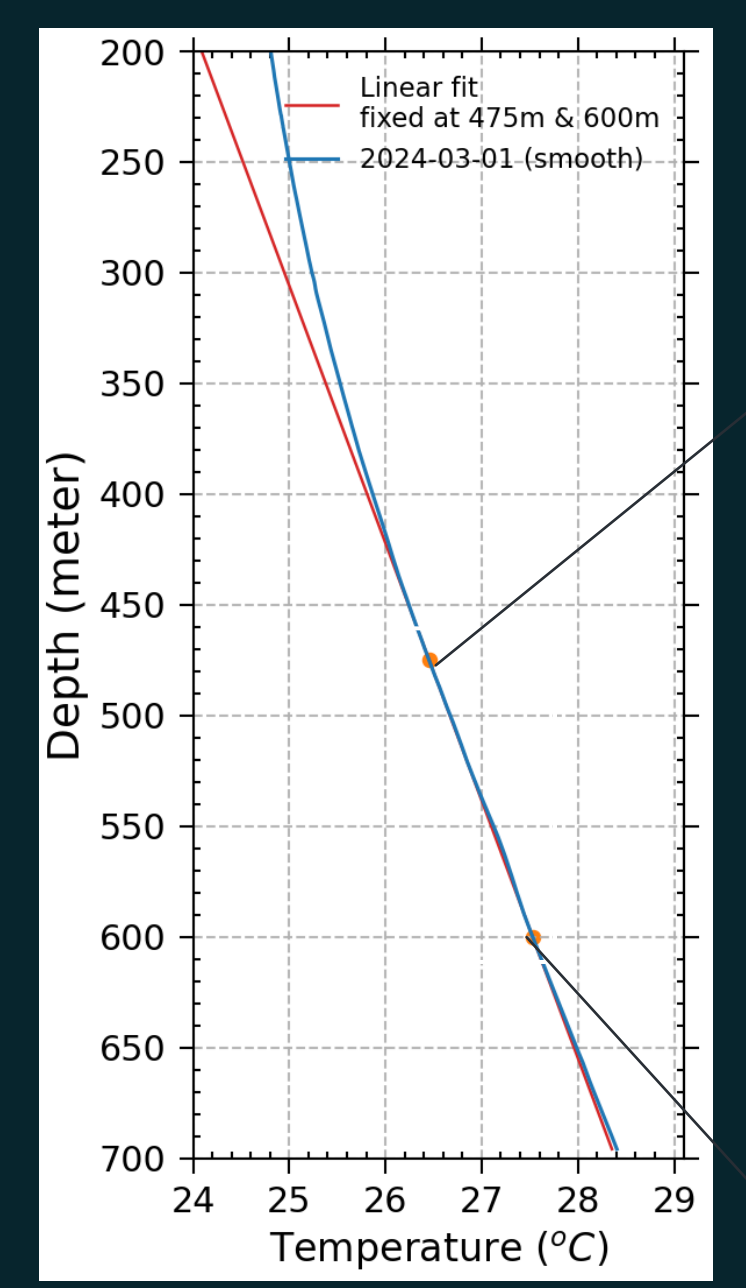




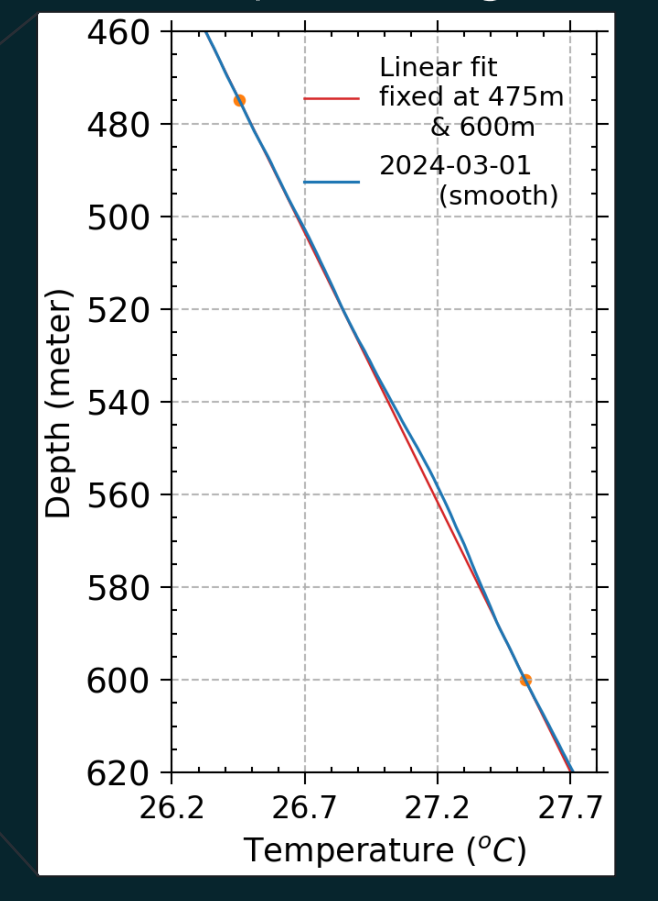


b 440.00

Persistent Thermal Anomaly

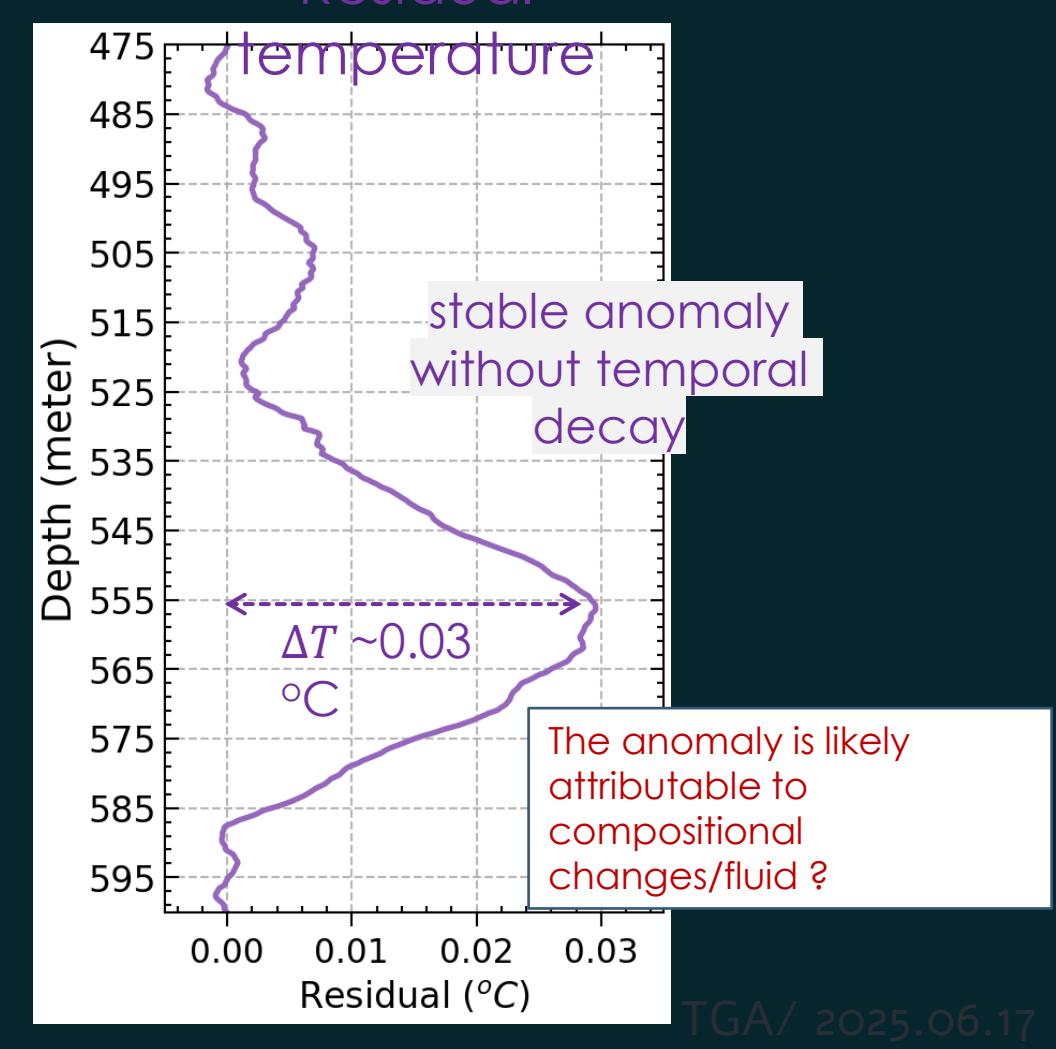


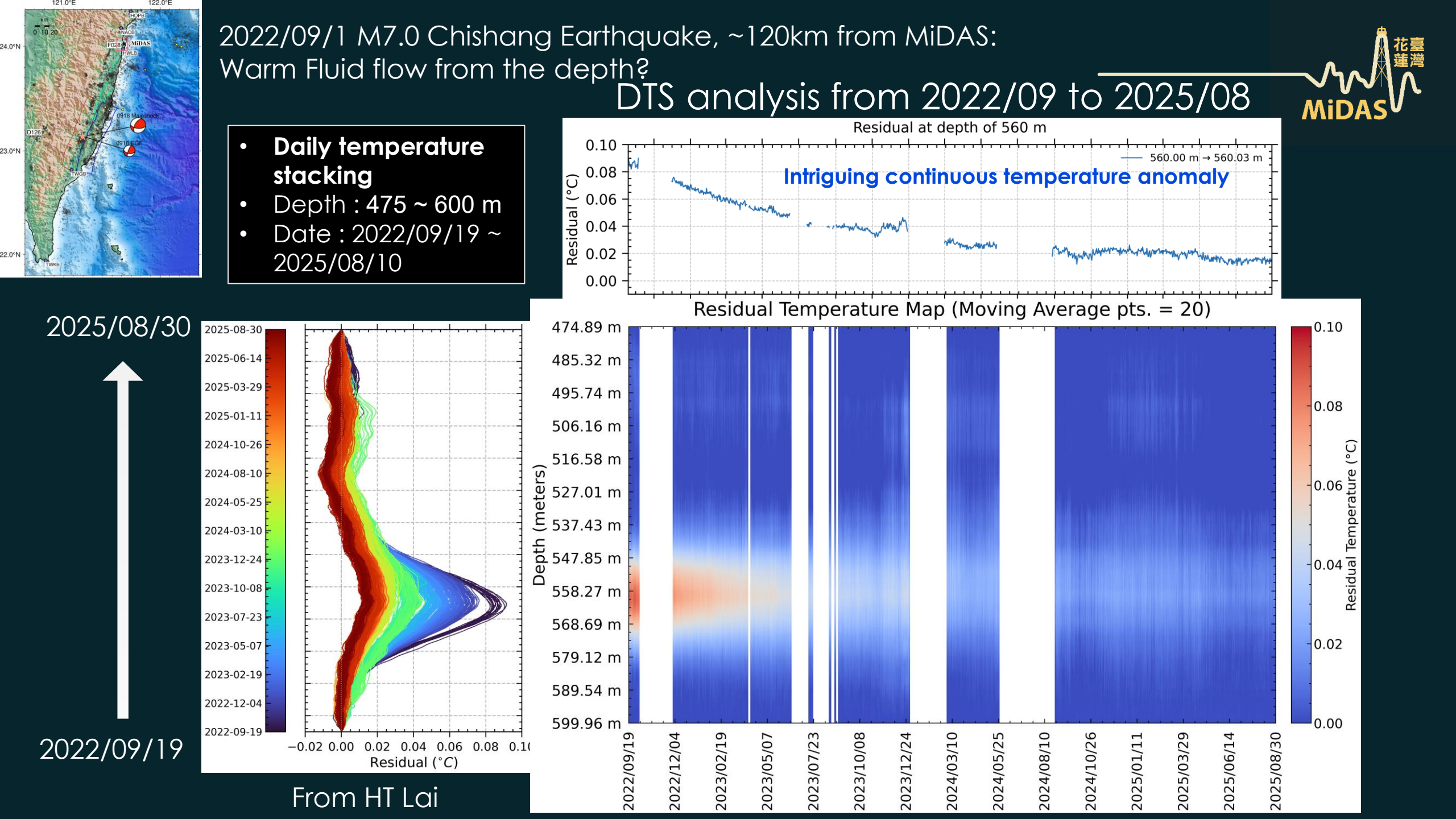
2024/03/01 Daily stacking



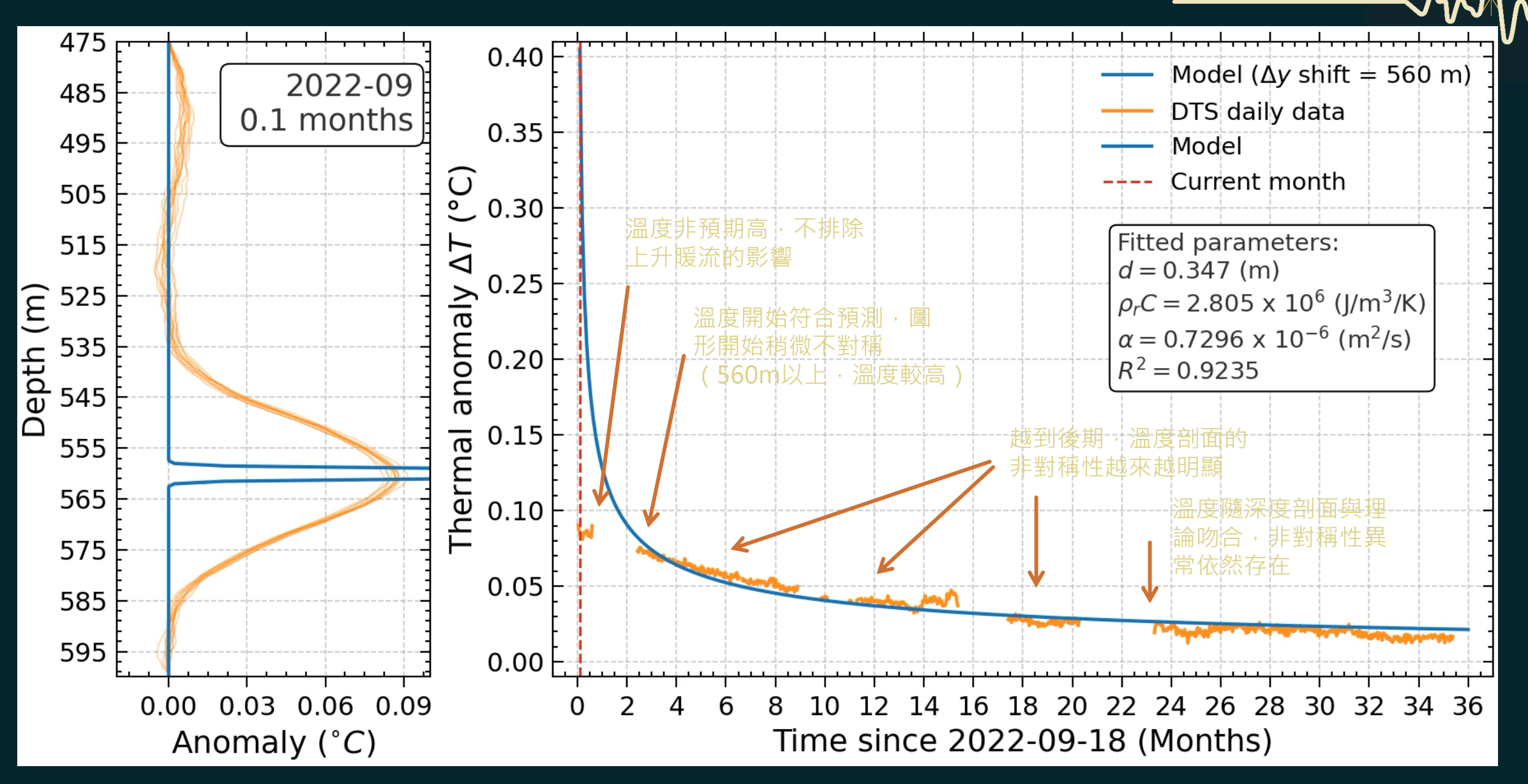
- Daily temperature stacking
- Depth resolution: 0.254 m
- Temperature resolution ~ 0.01 ° CDAS
- Moving average = 4.826 m (pts=20)

Residual





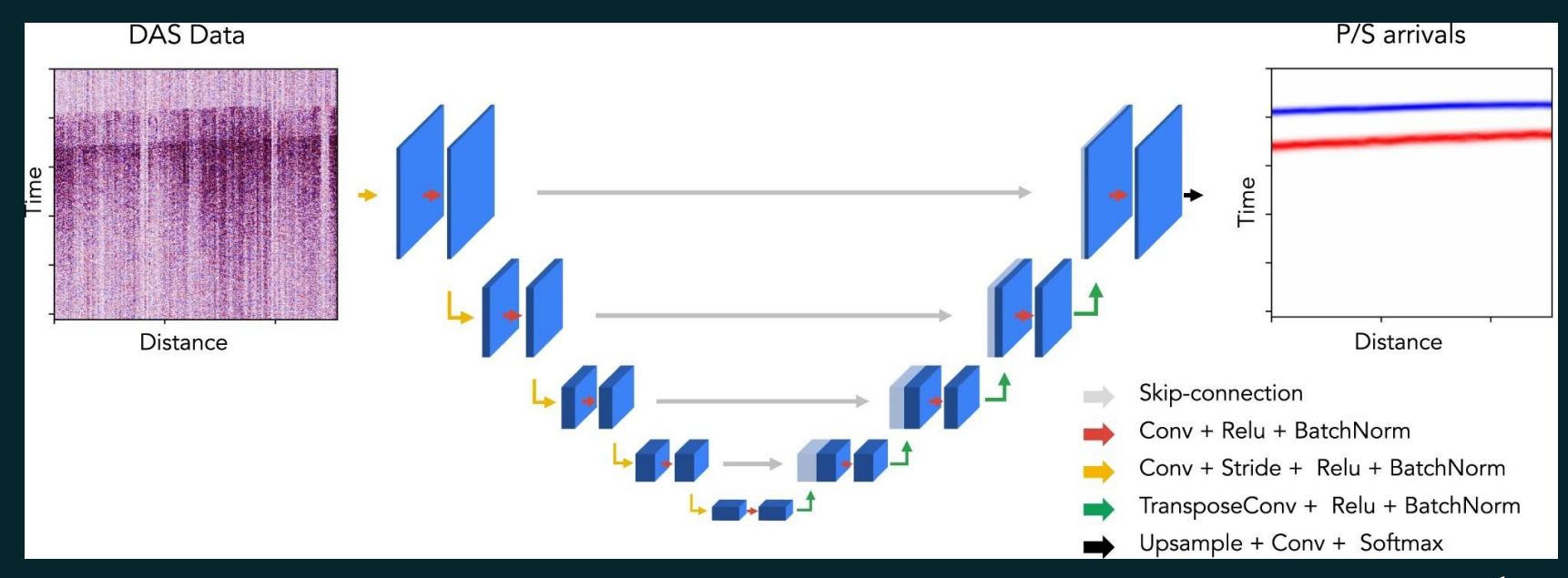
With hydrostatic pressure (Wet condition)



DAS BIG DATA=> AI APPLICATION FOR SEISMICITY INVESTIGATION

- * Exploring the application of Phasenet-DAS to continuous optical fiber DAS recordings of MiDAS
- * Convolutional neural network designed to pick P and S wave arrivals in DAS data
- Uses data from the MiDAS project. February 2023; Boreholes A and B (separately)
 - Notes: DAS data is noisier than seismometer data (especially surface DAS data)

 Typical methods don't leverage the extremely high spatial density of DAS



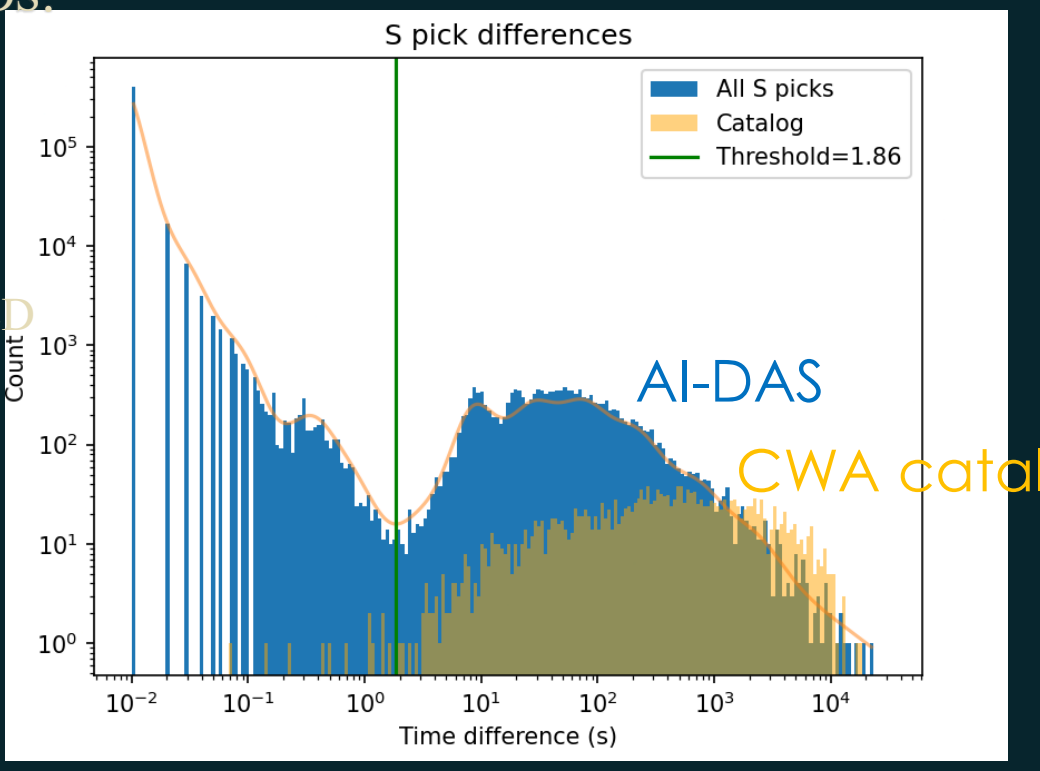
Trained on surface data from fiber-optic cables in Long Valley and Ridgecrest, California

Zhu et al. (2023)

ONE MONTH CONTINUOUS DATA (~20TB)_

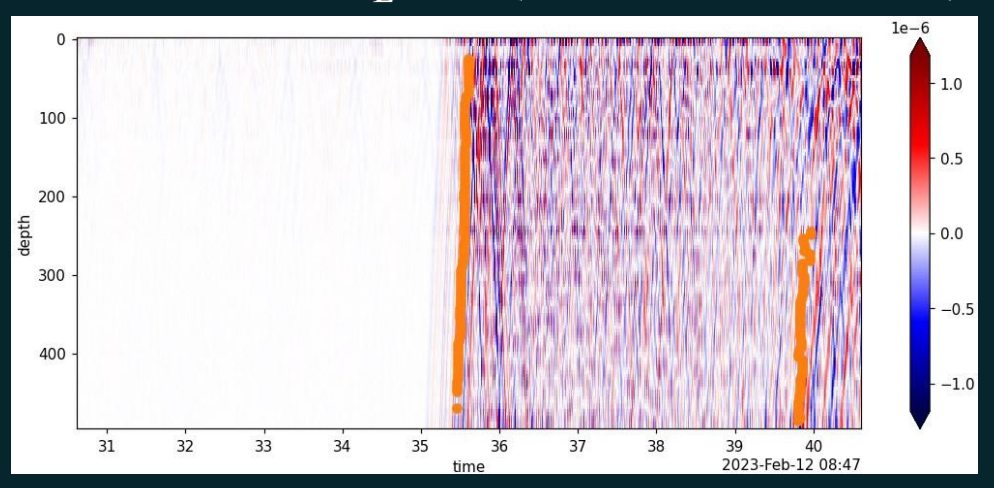


- PARTITION INTO 30 MINUTE LONG SECTIONS (NO OVERLAP)
- BANDPASS INTO ONE OF 15 DIFFERENT FREQUENCY BANDS:
- Lower frequency in 0.01, 0.1, 1 Hz
- UPPER FREQUENCY IN 10, 20, 30, 40, 50 HZ
- PHASENET-DAS WITH DEFAULT PROBABILITY THRESHOL (0.5)
- RAN FOR ABOUT A WEEK ON A SINGLE SERVER
- => Originally split picks into events with at least 1.86 second time difference (only differentiating boreholes)
- => Threshold picked based on histogram of time differences

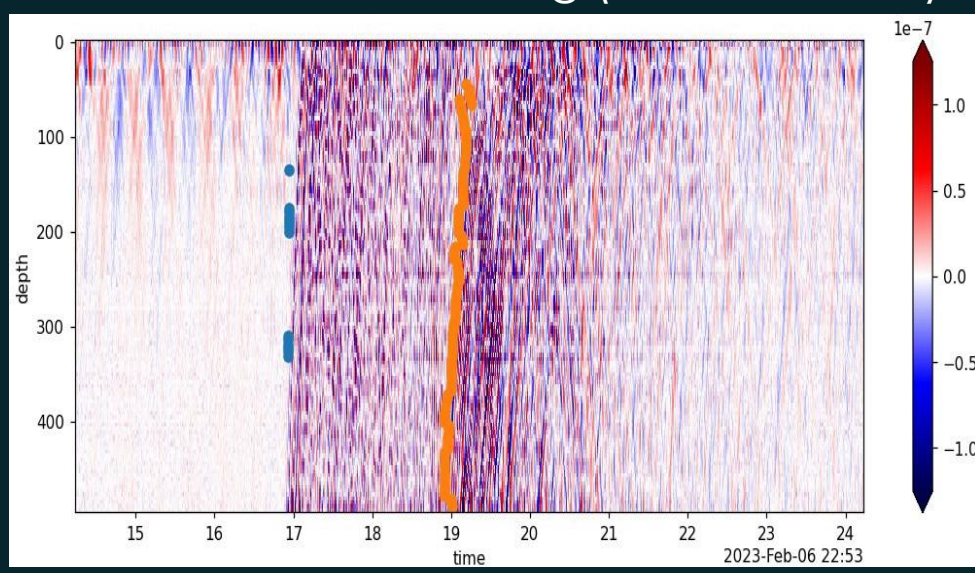


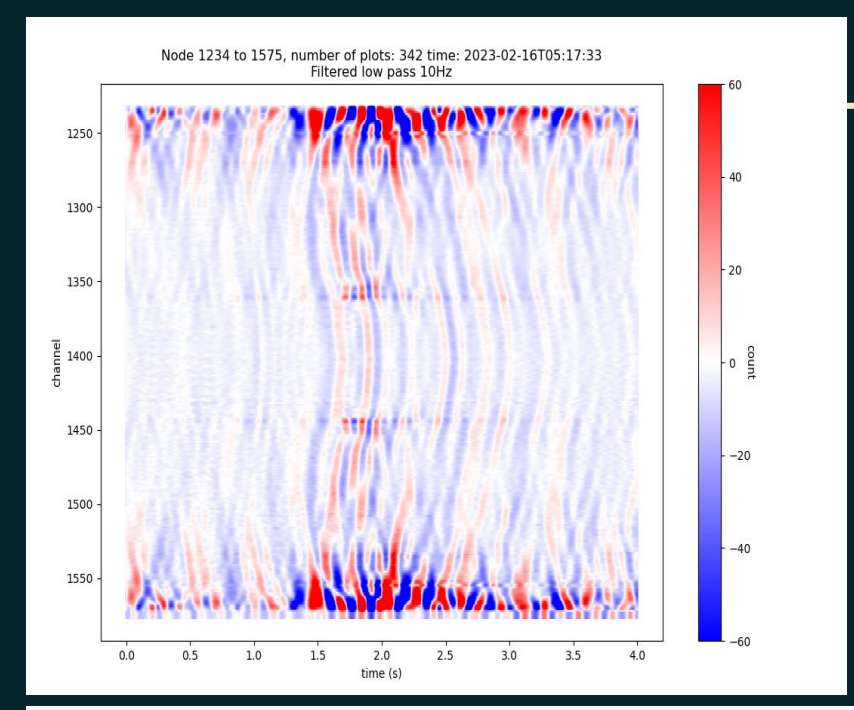
- * Log-Log histogram of time between adjacent picks
- * It is also possible using slope as an event identifier.

5 KM AWAY M_L 3.44 (CATALOG EVENT)



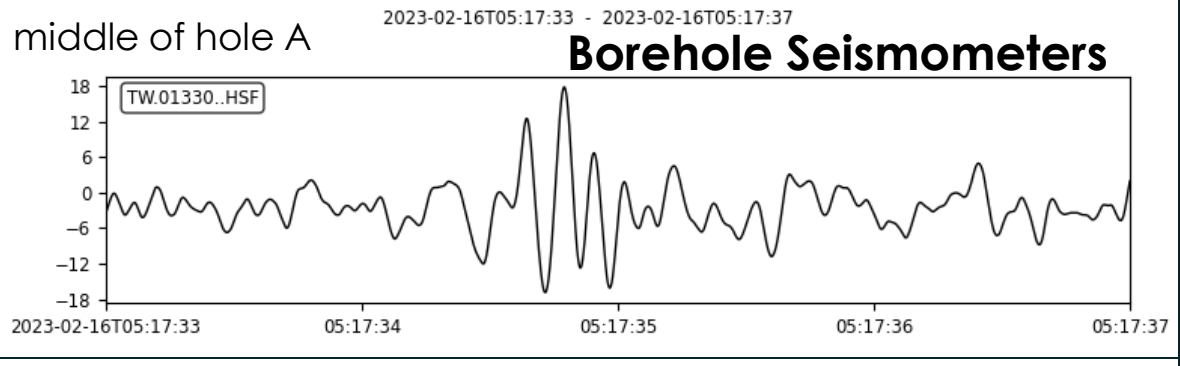
Event not in the catalog (20230206~M0)

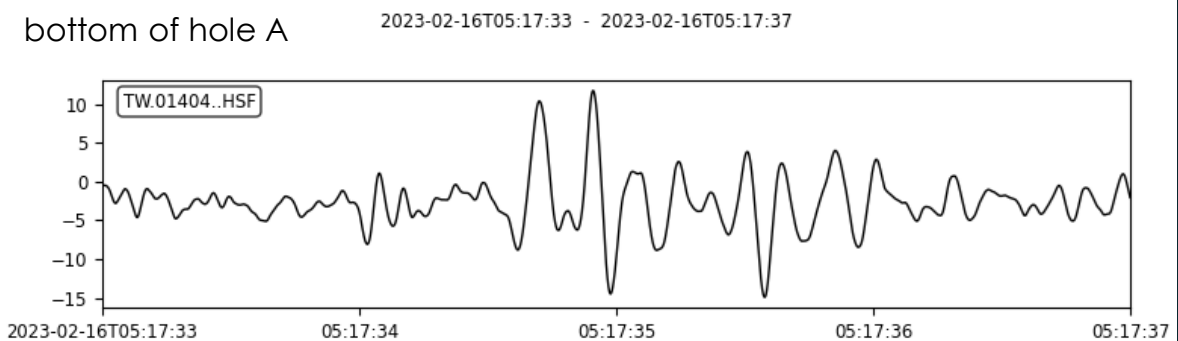






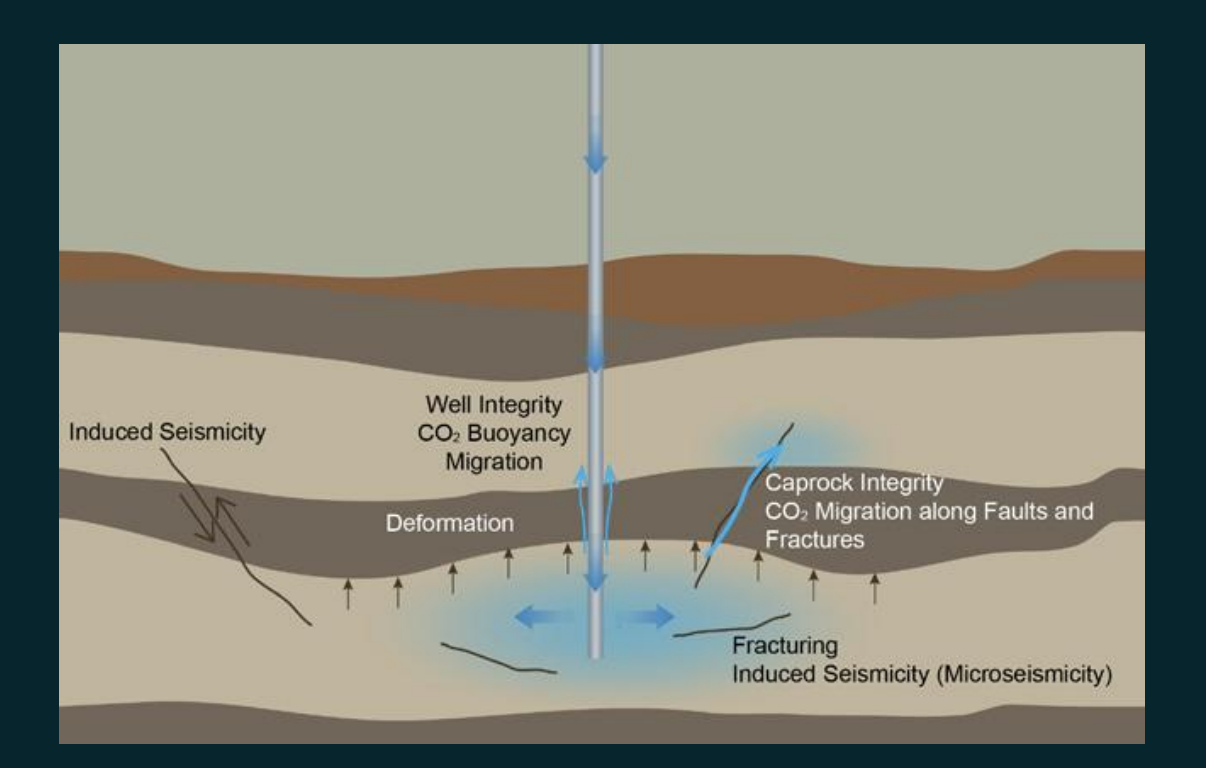
Very close-by shallow possibly hydraulic event (M~-1)





By Yen-Yu Lin

Processes during active CO2 injection (Rutqvist, 2012)



- Well integrity: leakage of CO2 upward to shallow aquifers or the surface.
- Migration of CO2 along faults and fractures
- Migration of CO2 plume outside of the storage reservoir
- Induced seismicity:

Silixa, Carbon Capture and Storage Monitoring with distributed fiber optic sensing, (March, 2022)



How Borehole DAS/DTS Observations at the MiDAS Site Can Help:

- Borehole DAS (Distributed Acoustic Sensing) and DTS (Distributed Temperature Sensing) technologies offer high-resolution, real-time data for enhanced monitoring.
- These methods improve understanding of subsurface dynamics before, during, and after the injection period.

Key Insights for Future Applications:

- Fiber optic distributed sensing significantly enhances spatial and temporal data resolution.
- Lessons learned from the MiDAS site can guide the development of advanced monitoring techniques for injection-related processes, ensuring more effective characterization and management of subsurface systems.

FIBER DATA FOR MAGNITUDE DETERMINATION

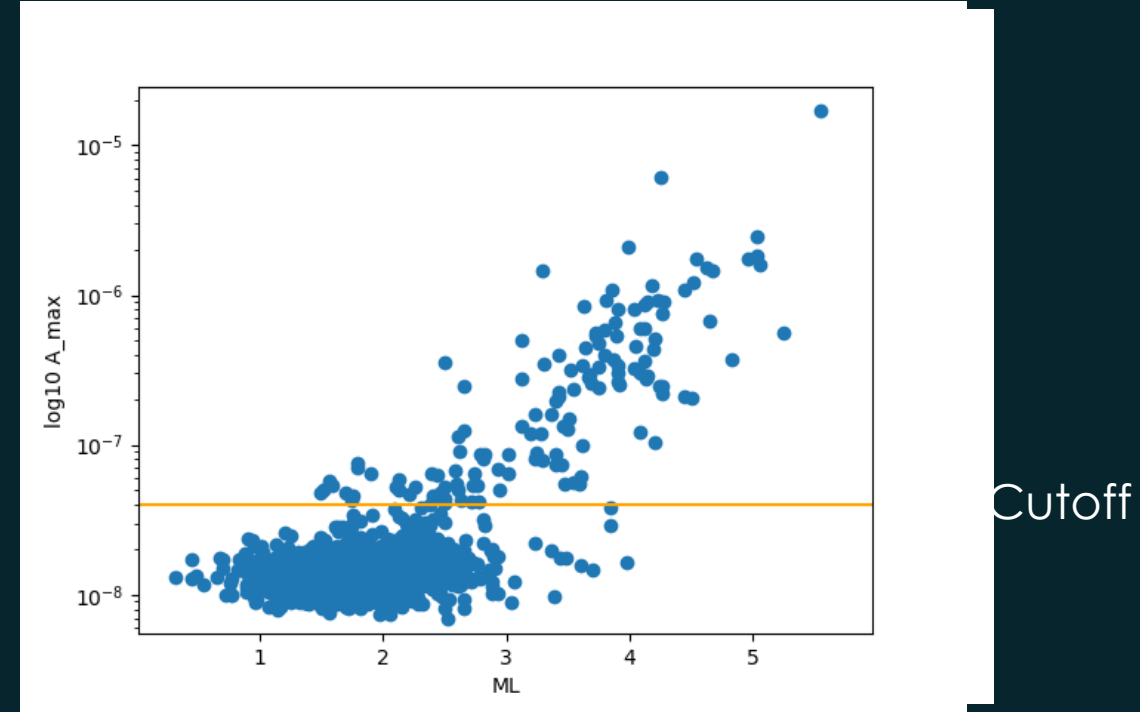


DATA USED

- CWA CATALOG FOR MONTH OF JUNE 2024 AS WELL AS FIRST WEEK OF MAY 2025 WERE USED
- FILTERED OUT EVENTS WITHIN 3 MINUTES OF EACH OTHER

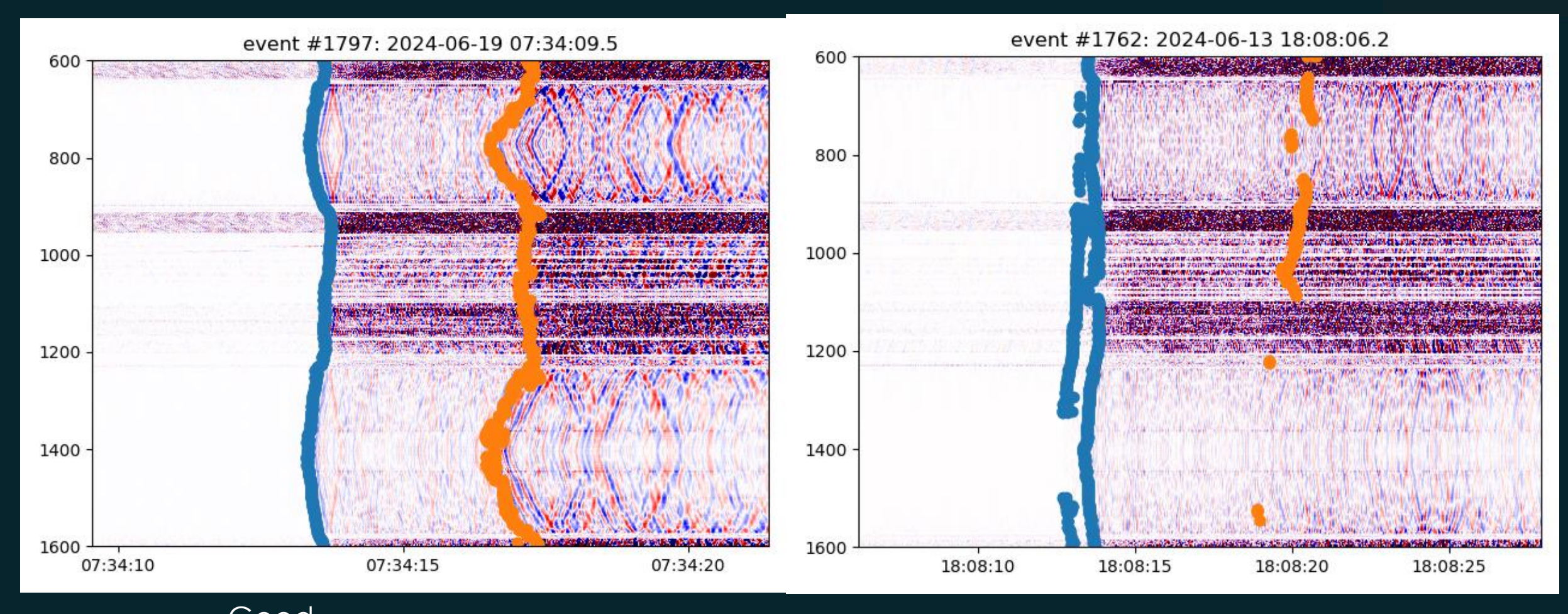
• PLOT OF ML vs A_max revealed noise was around 7e-9 to 3e-8 m/m/s so filtered out events with A_max < 4e-8

- EVENTS REMAINING WERE PROCESSED USING PHASENET-DAS AND MANUALLY FILTERED (SEE NEXT SLIDE)
- EVERYTHING FILTERED 0.1-20 Hz



GOOD AND BAD RESULTS FROM PHASENET-DAS





Good Phasenet-DAS run on entire fiber for 1 minute before to 2 minutes after the earthquake origin time. Results were then cut to only picks between the origin and twice the expected S-arrival time.

Bad

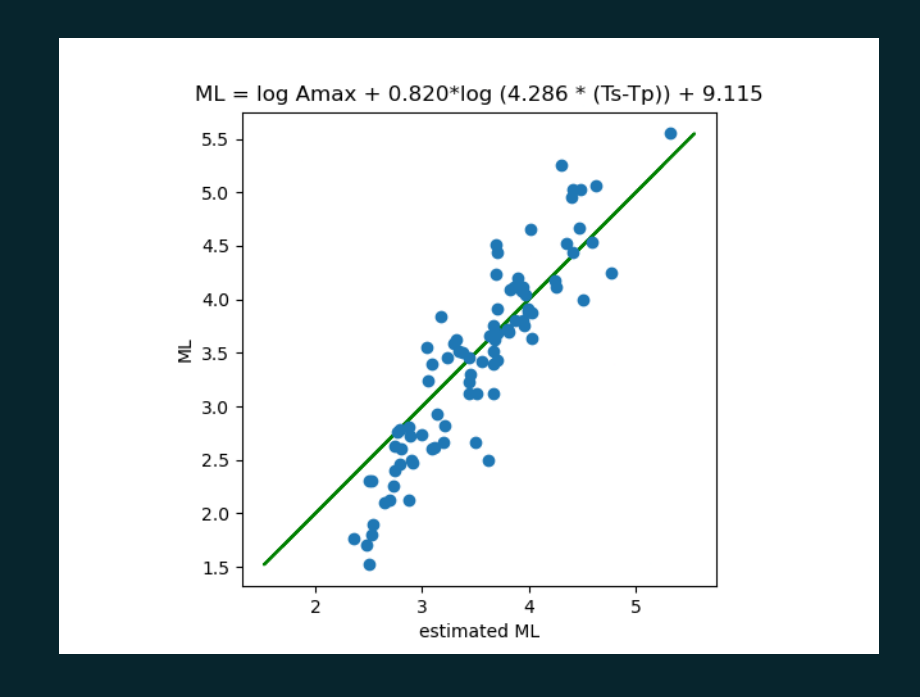
ESTIMATING ML USING AMPLITUDE AND TS-TP TIME

 $ML_{SR} = \log Amax + 1.888 \log(4.825*(ts-tp)) + 7.534.$

ML = log Amax + 1.888*log (4.825 * (Ts-Tp)) + 7.534used for regression 5.5 5.0 **≝** 3.5 3.0 2.5 2.0 1.5 estimated ML ML_{SR}

(Amax: strain rate, m/m.sec; ts, tp: sec)

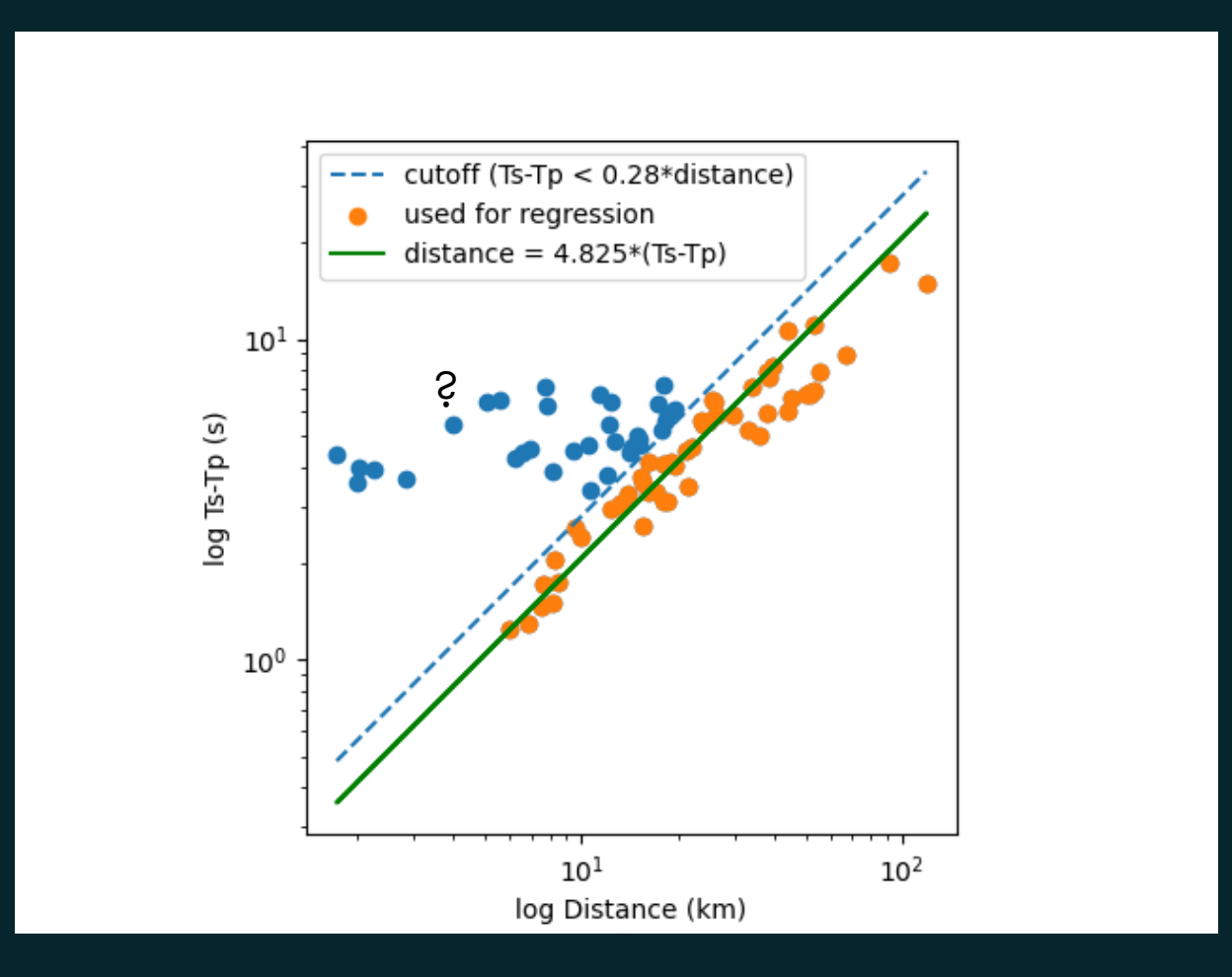
Use ts-tp time to estimate distance, and then use that distance and the max amplitude to estimate magnitude

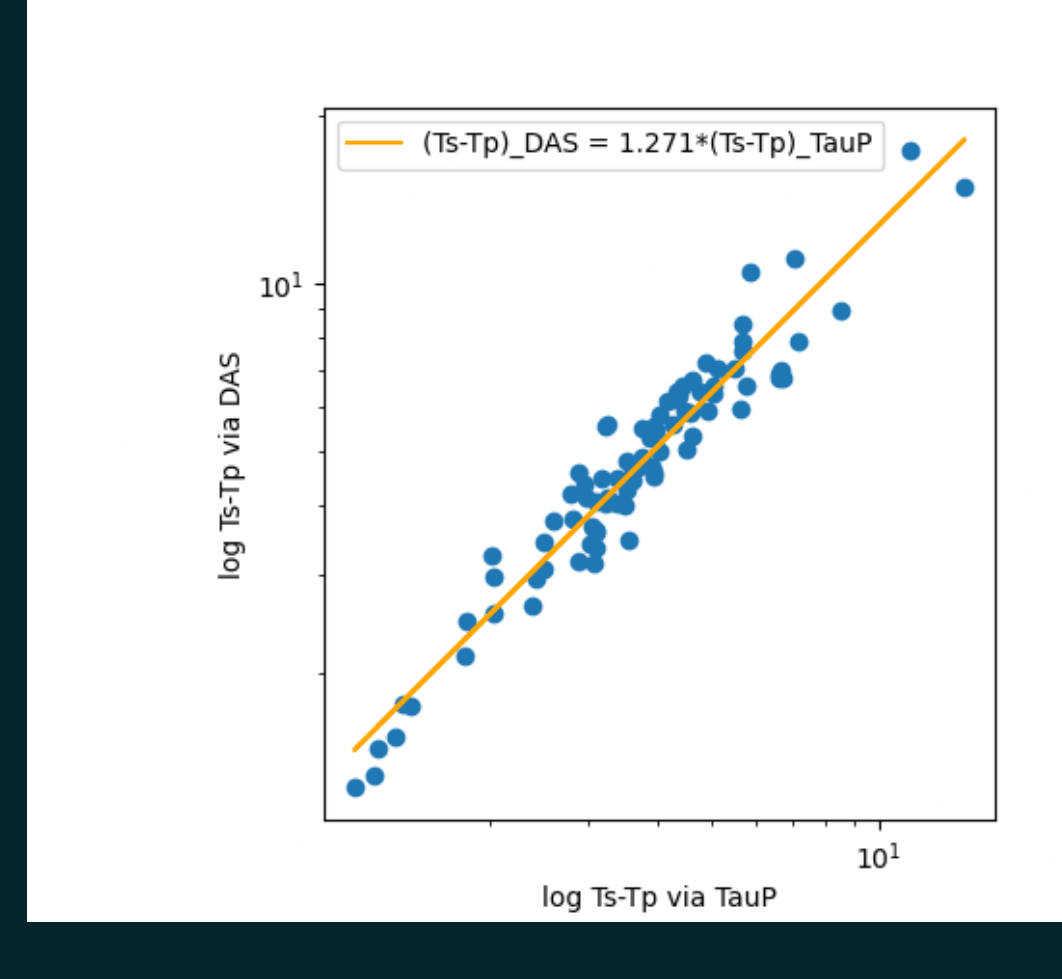


If using regressions based on all points

ESTIMATE DISTANCE FROM TS-TP TIME (HOLE-A, JUNE CATALOG EVENTS)





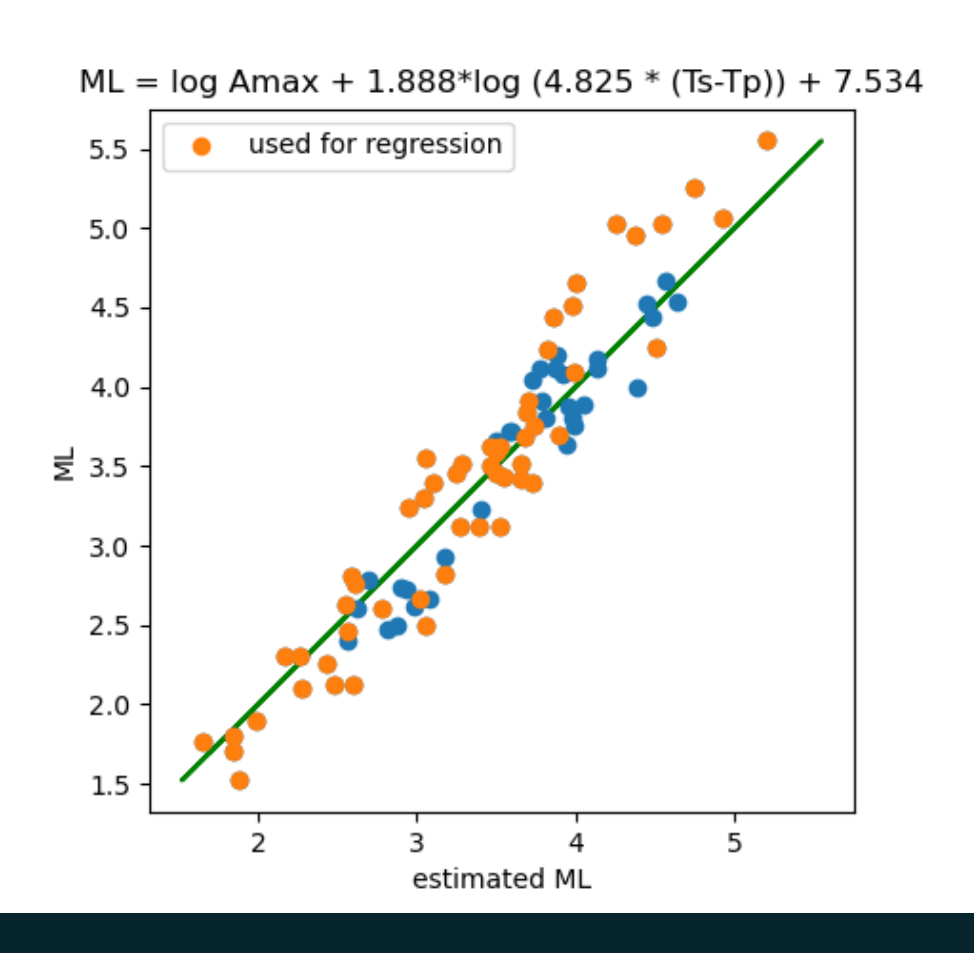


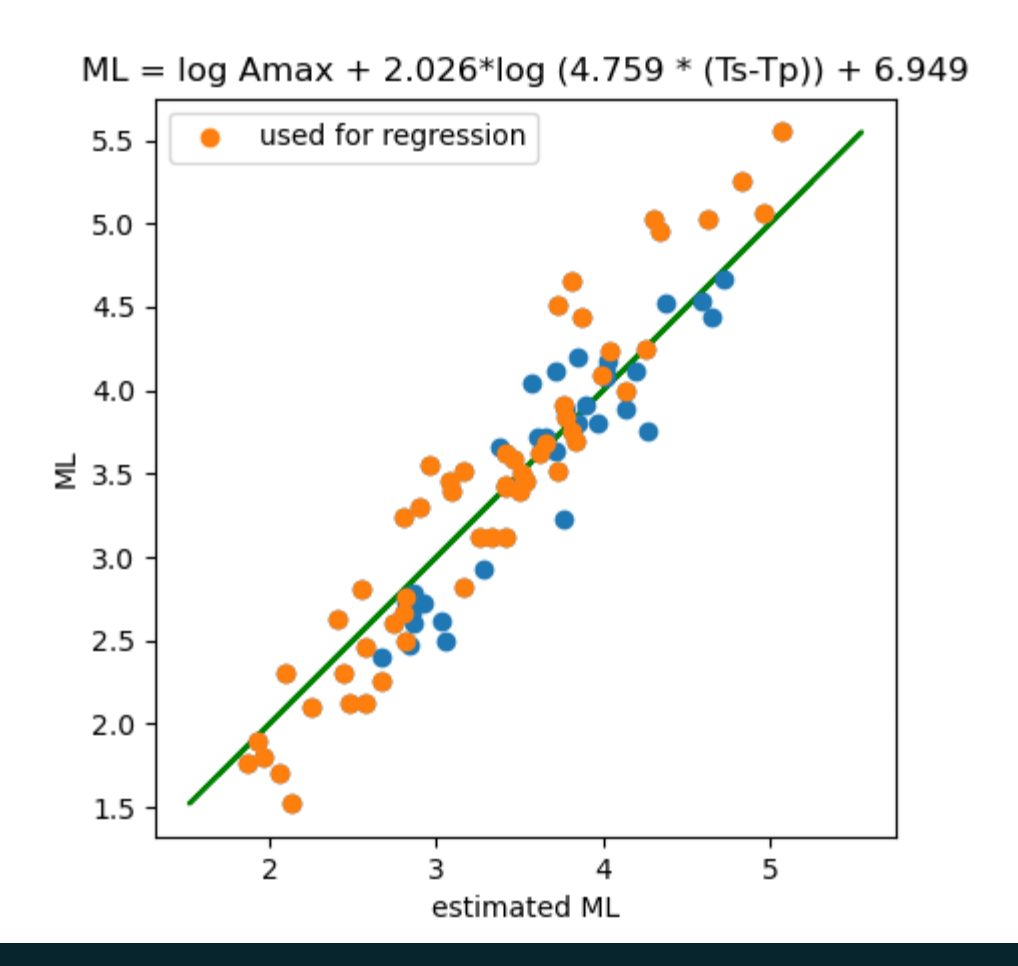
Points in orange are used for all other regressions

COMBINED REGRESSION HOLE A VS HOLE B



Hole A Hole B



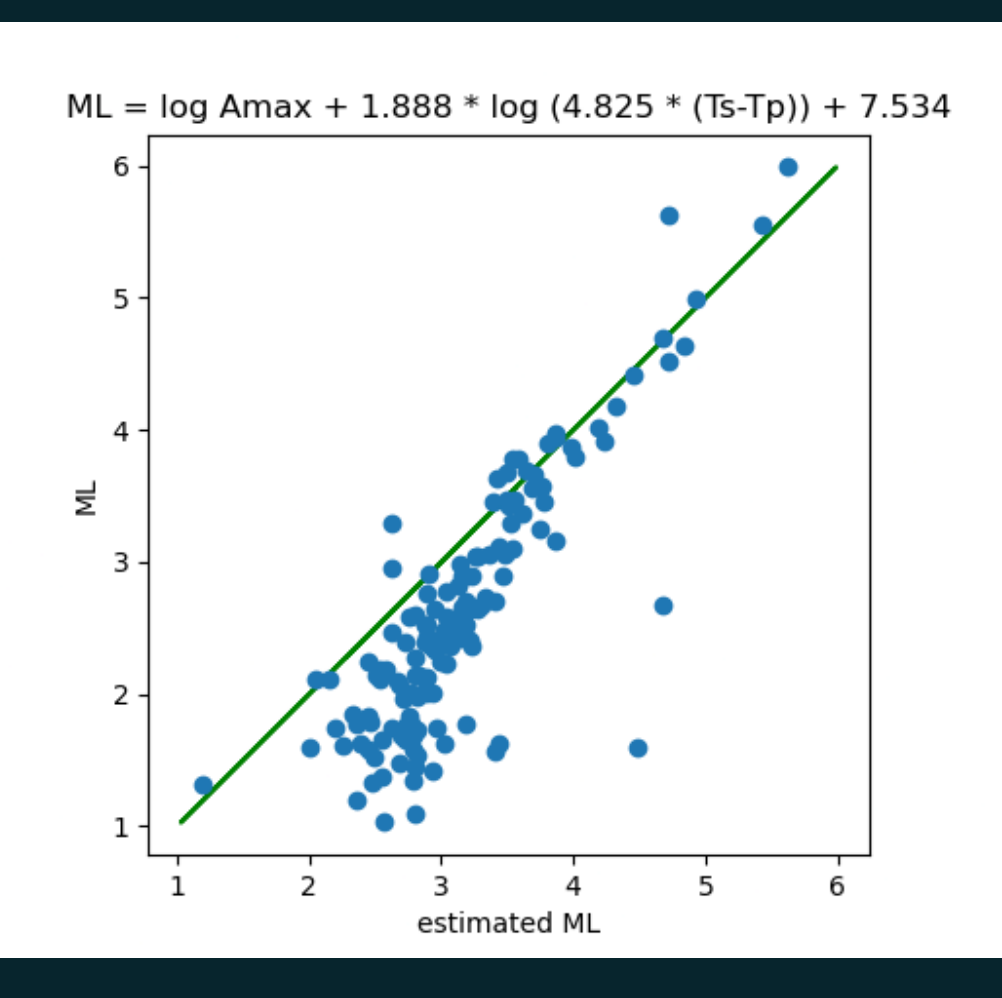


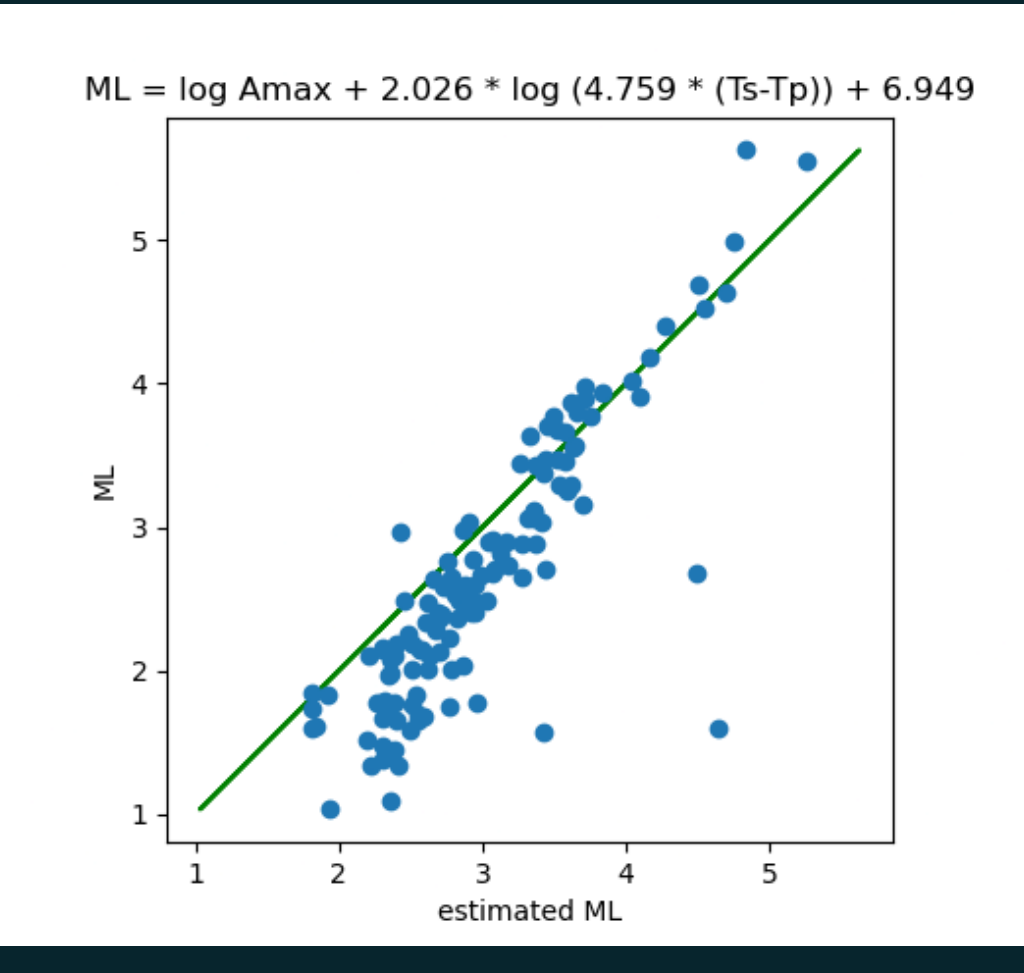
TESTING REGRESSION ON MAY, 2024



Hole A

Hole B

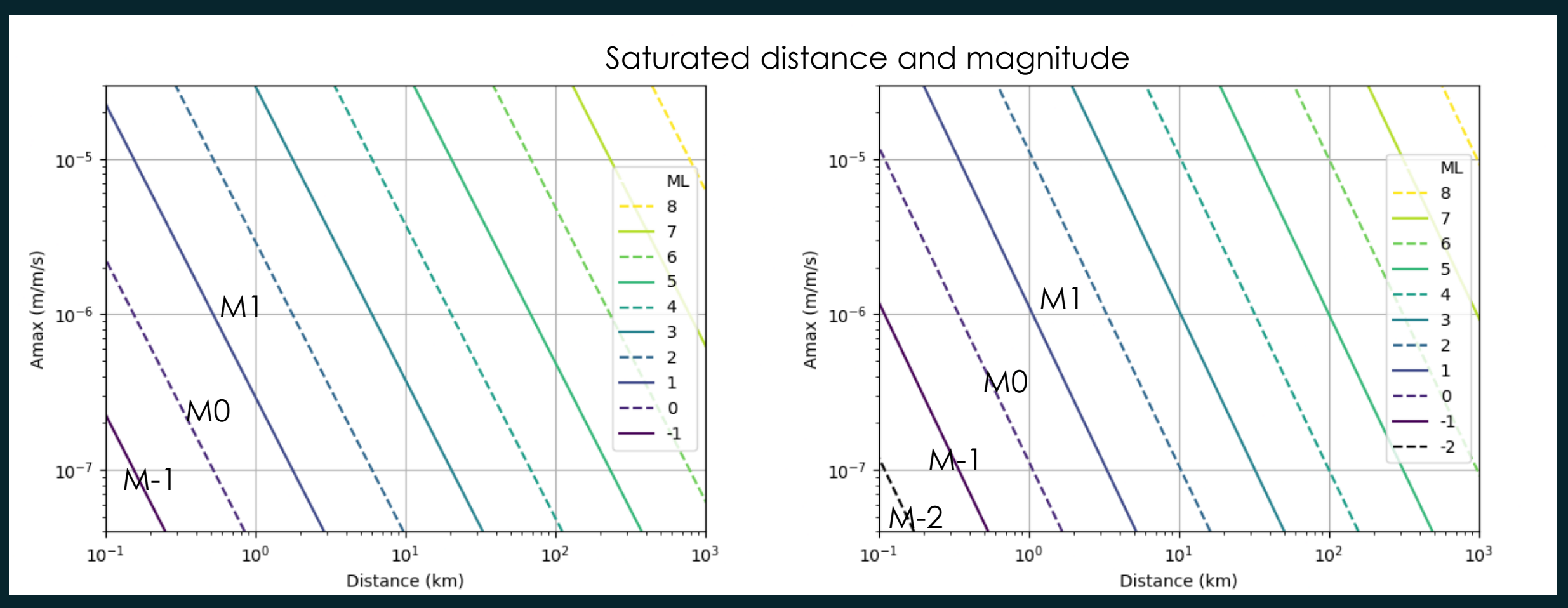






CAPABILITY HOLE A VS HOLE B

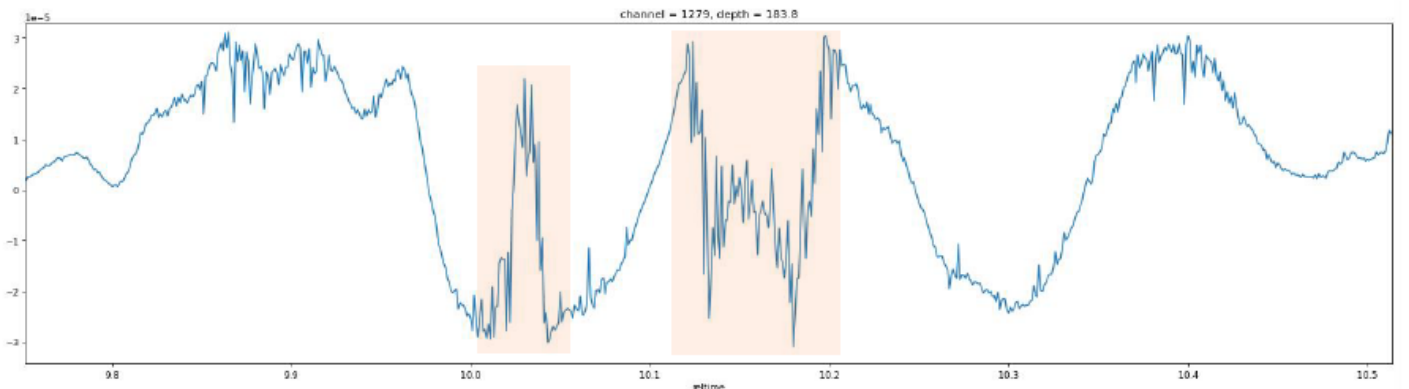
Amplitude limits are noise floor (~4e-8) and saturation point (~3e-5)



What's the issue with wrapping?

Phase shift is by definition measured in a limited range from $-\pi$ to π , but strain rate is not so limited.

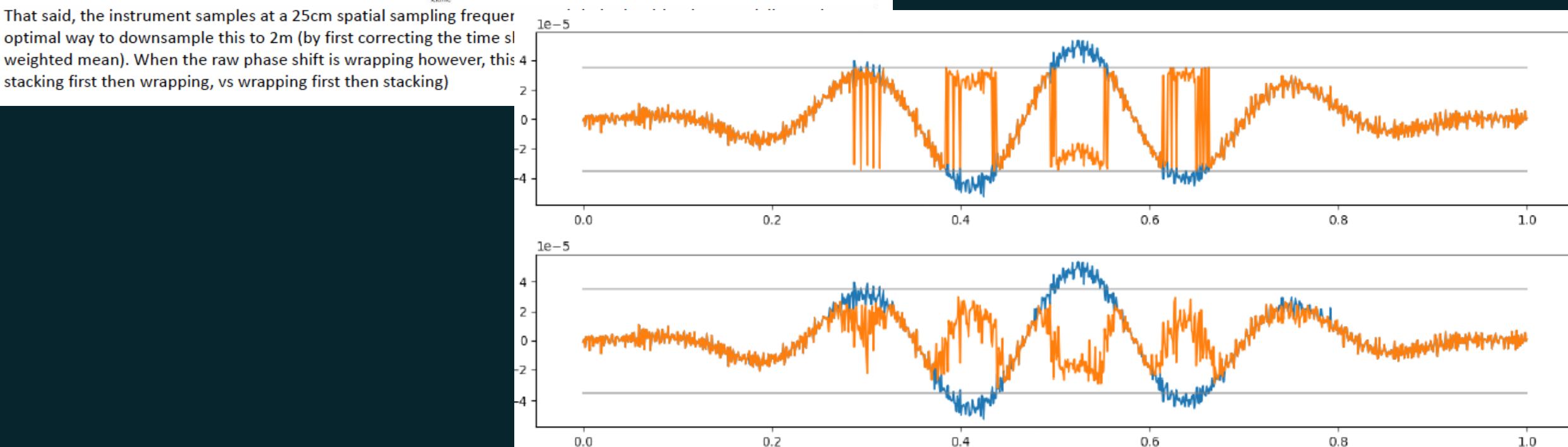
Normally this wouldn't be an issue (methods dealing with e.g. inSAR data would work), however in our case the instrument uses some proprietary denoising algorithm on the raw data, which has the side effect of mostly eliminating the large jumps that usually characterize wrapped phase data. (The shaded boxes below indicate wrapping sections)



"Saturation" Issue for Strong Motion

Wrapping/Unwrapping*

By Alexander Ristich

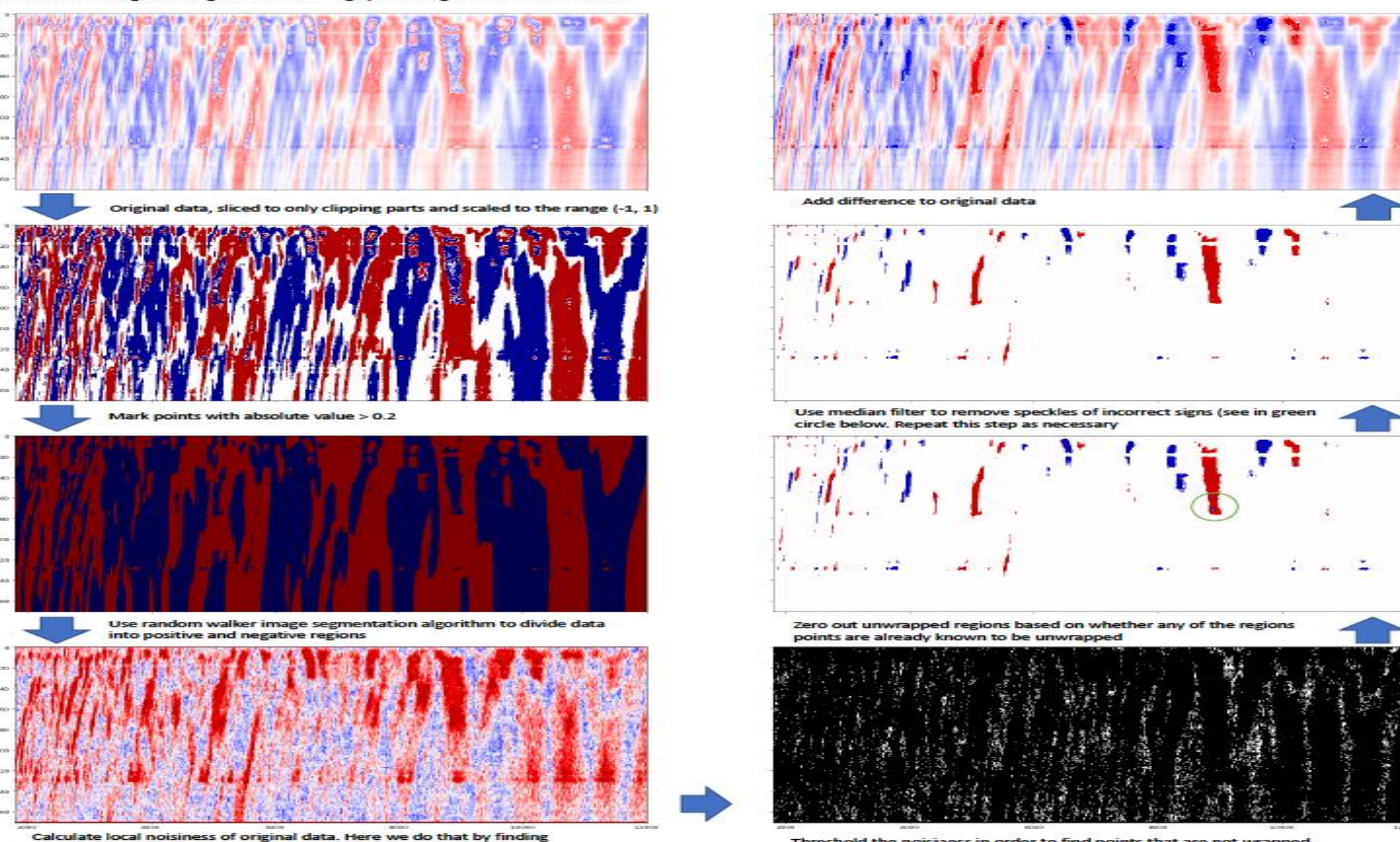


Method

a best fit paraboloid to a pixel and its 8 neighbors, and output the

squared sum of differences

Note that wrapping occurs in more or less contiguous regions. We should be able to unwrap the data by simply adding or subtracting a constant value to those regions. So the problem become discounting the same regions are the same regions. So the problem become discounting the same regions are the same regions.

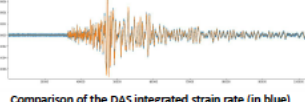




Verification

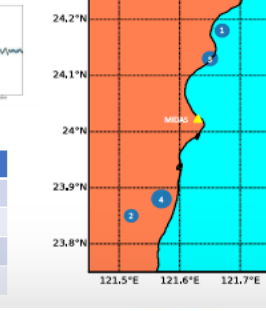
In order to verify our results we can compare the unwrapped data to seismometer data. The way we do that is the integral of strain rate from 100m to 695m in hole A should be equivalent to the difference in vertical velocities at those points.

While in theory these should be equal, in practice we scale the seismometer data by about 0.7 (parameters found by least squares fit with a small earthquake).



Comparison of the DAS integrated strain rate (in blue) and the acceleration derived strain rate (in orange)

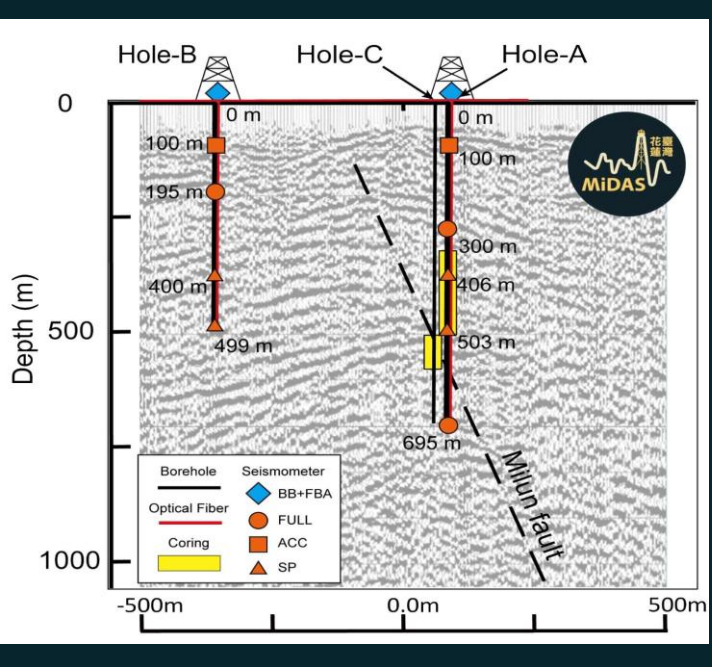
	UTC Date/time	Magnitude	Latitude	Longitude	Depth (KM)	Distance (KM)	
1	2024-04-26 18:21:24	6.3	24.18° N	121.67° E	35.5	39.7	
2	2024-04-22 18:32:48	6.2	23.85° N	121.52° E	7.7	23.5	
3	2024-04-03 00:11:26	6.5	24.13° N	121.65° E	13.4	18.0	
4	2024-04-02 23:58:09	7.1	23.88° N	121.57° E	19.7	26.0	



Recovering of the wrapping signals On-going test with borehole seismometers (Alexander Ristich)

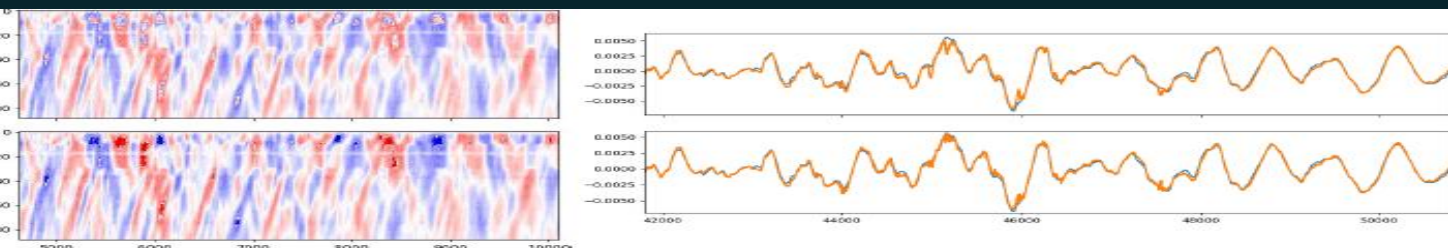


Borehole seismometers/ Optical fiber strain rate



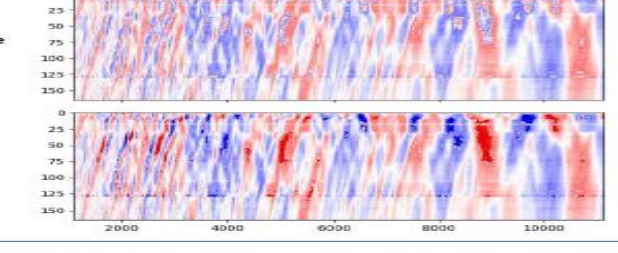
#1 Minimal Clipping

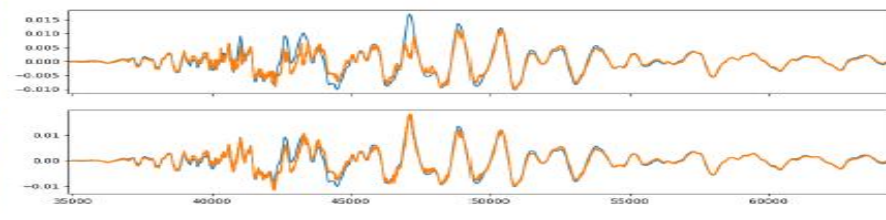
Looking at the waterfall plot, it appears to work, although there is very little difference in the



#2 Some clipping

eveal any issues, and this time there is a much more noticeable (especially around 40000)

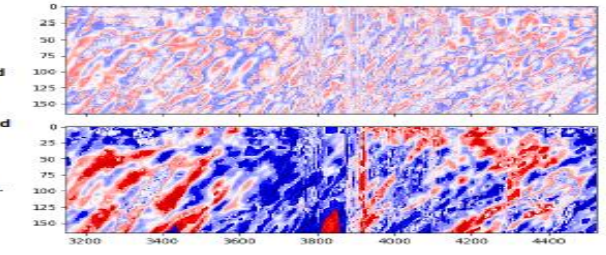


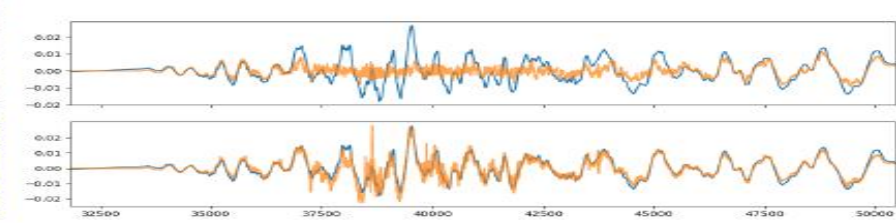


#3 Strong clipping

oticeable issues from the waterfall ncorrected, and a region near the

n the other hand, the comparison ows a pretty striking improve

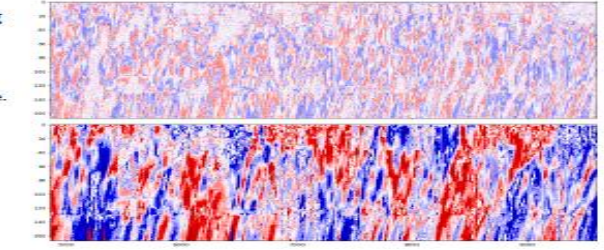


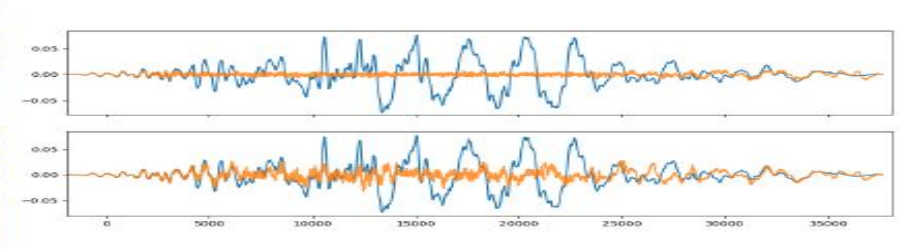


#4 Very Strong clipping

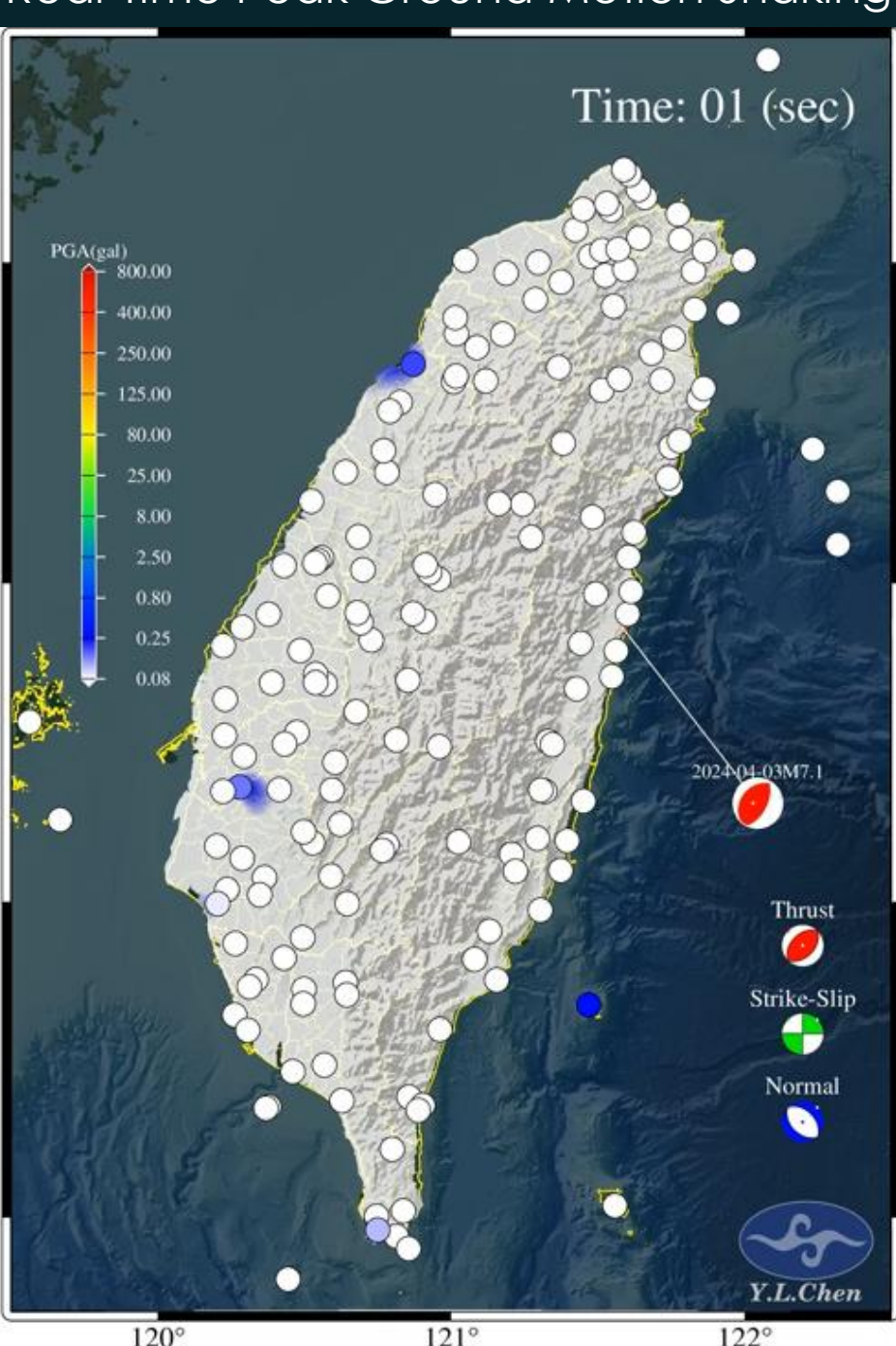
Regarding the main shock, the

The comparison also indicates the around 3x range increase achievable

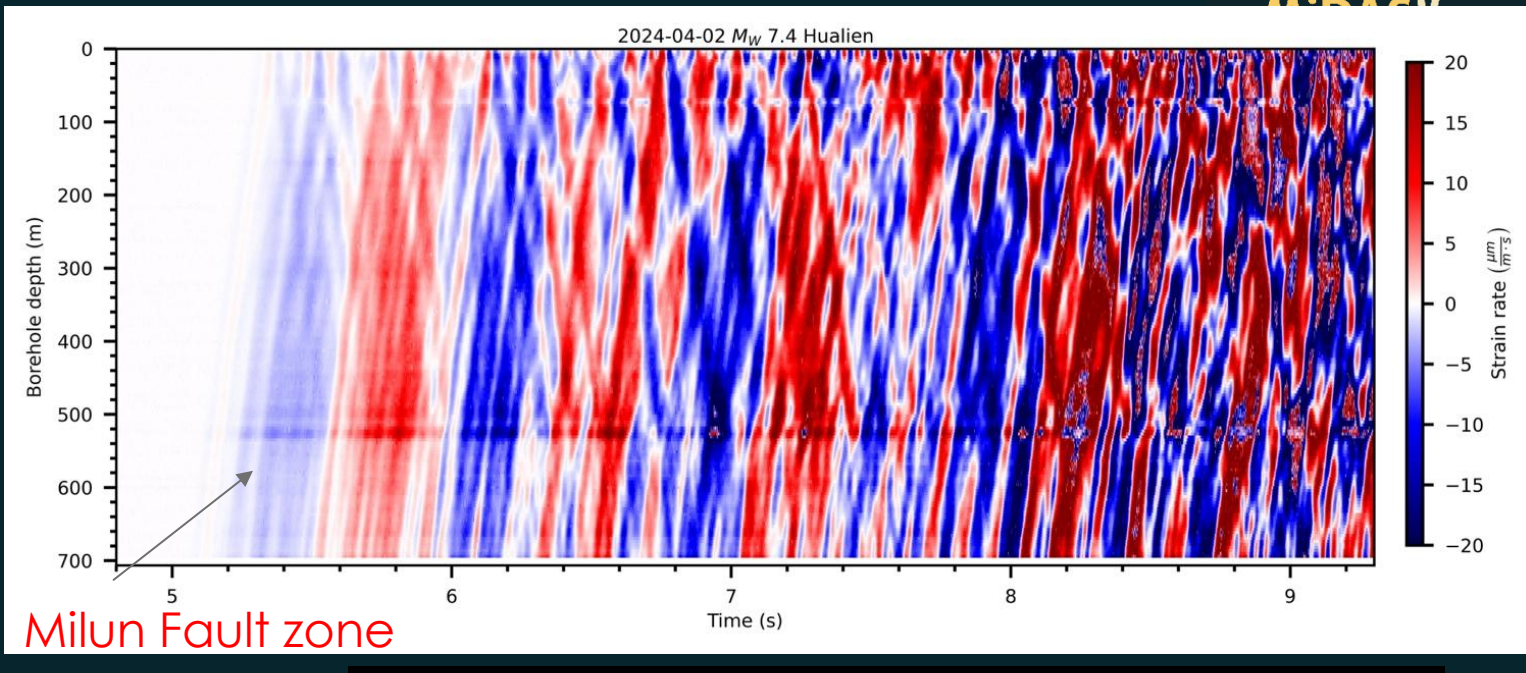




Real-Time Peak Ground Motion Shaking



20240403 M7.2 earthquake (Hole-A) @MiDAS (20 km away from MiDAS site)



The time it shakes @MiDAS (PGA ~250 gal, permanent uplift, ~30cm)

Summary

- Well integrity: leakage of CO2 upward to shallow aquifers or the surface.

- Migration of CO2 along faults and fractures
- Migration of CO2 plume outside of the storage reservoir
- Induced seismicity:
- DAS/DTS Emerging technology for ultra-fine structure spatial and temporal mapping
- Broadband strain amplification directly related to the reduction in elastic modulus, namely the rigidity (μ) .
- Good indicator for fluid flow monitoring (or gaseous and liquid carbon dioxide).
- Continuous spatial resolution of DAS data provide real-time seismicity mapping using AI. Together with geophone and borehole seismic array for locations.

Key Insights for Future Applications:

- Fiber optic distributed sensing significantly enhances spatial and temporal data resolution.
- Lessons learned from the MiDAS site can guide the development of advanced monitoring techniques for injection-related processes (geothermal, CCS...), ensuring more effective characterization and management of subsurface systems.

Milun fault Drilling and All-inclusive Sensing 人人 MiDAS observatory at beautiful Chishintan (七星潭) MIDAS





